Available online at www.sciencedirect.com
SCIENCE DIRECT®
Coordination Chemistry Reviews 238–239 (2003) 363–382
COORDINATION CHEMISTRY REVIEWS
www.elsevier.com/locate/ccr

The importance of interligand interactions to structure and reactivity of coordinatively unsaturated ruthenium and iron half-sandwich complexes—application of the TSC concept II

Valentin N. Sapunov [b], Roland Schmid [a,*], Karl Kirchner [a], Hideo Nagashima [c]

[a] *Institute of Applied Synthetic Chemistry, Vienna University of Technology, Getreidemarkt 9, A-1060 Vienna, Austria*
[b] *D. Mendeleev University of Chemistry and Technology of Russia, Miusskaja 9, 125047 Moscow, Russia*
[c] *Institute of Advanced Material Study, Kyushu University, Kasuga, Fukuoka 816-8580, Japan*

Received 4 March 2002; accepted 5 September 2002

Contents

Abstract

The interaction between any fragments bonded to some central atom are increasingly recognized as an important factor in determining, e.g. the geometry and properties of metal complexes. Here we analyze the class of the two-legged piano stool complexes $Cp'ML_2$ (Cp' = cyclopentadienyl or a derivative, M = Fe(II) and Ru(II), L = phosphorus and nitrogen co-ligands) with the aid of the through-space coupling (TSC) concept. This is the molecular orbital representation of van der Waals-like repulsive–attractive forces between the ligands in addition to the interactions with the metal center. The combination of both, i.e. the interaction between the new collective ligands orbitals and the metal AO's is shown to be the main determinant for deciding whether a planar or pyramidal structure is adopted and further, whether the complex is diamagnetic or paramagnetic. In addition the TSC concepts aids in understanding the effect of intercomplex interactions on the nucleophilic and electrophilic behavior of the 16e-complexes towards

* Corresponding author. Tel.: +43-1-5880115340; fax: +43-1-5880115499
E-mail addresses: vals@muctr.edu.ru (V.N. Sapunov), rschmid@mail.zserv.tuwien.ac.at (R. Schmid), kkirch@mail.zserv.tuwien.ac.at (K. Kirchner), nagashima@cm.kyushu-u.ac.jp (H. Nagashima).

PII: S0010-8545(02)00255-2

an incoming ligand. In fact, interpretations hitherto solely in terms of electronic ligand effects appear to be inadequate. The present paper is a continuation of our former work in which we successfully applied the TSC concept to rationalize the diverse array of structural arrangements as well as reactivities of the main-group Cp metal complexes (Sapunov et al. Coord. Chem. Reviews 214 (2001) 143).

Keywords: Bond theory; Coordination chemistry; Through-space interactions; Ruthenium; Iron; Half-sandwich complexes

1. Introduction

The application of transition metals to organic synthesis and catalysis has been one of the most active research areas in organic chemistry over the past decades [1]. The progress which has been achieved in the field of synthetic organometallic chemistry is of course also based on the increased *know how* in the handling of very sensitive organometallic compounds on a scale useful for new synthetic purposes [2]. Transition metals in complexed form have especially been playing a pivotal role in this tremendous development. The large majority of the complexes used as catalysts adhere to the 18-electron (18e) rule, and can as such, of course, not to be catalytically active without transient conversions. Since the intervening intermediates are often elusive, the mechanistic details of many catalytic cycles remain unclear and uncertain. Hence, mechanistic suggestions are often based more on intuition or preconceived opinion than on experimental evidence. For further advancement it is worthwhile to focus on the study of the few, but increasing in number, known relatively stable 'genuine' 16e-complexes. Among these, the paramagnetic species [3,4] are of particular interest because of their relevance to spin-forbidden conversions necessitating catalysts that are capable of spin conversion. Focusing on the structure and reactivity of such compounds will ultimately aid in understanding the mechanism of molecular rearrangement and transformations in the coordination sphere of complexes during a catalytic cycle or stoichiometric synthesis.

It is increasingly recognized that stoichiometry, coordination geometry, and reactivity of metal complexes are dictated not by the bonds between the metal and the atoms attached to it, but by the 'non-bonded' interactions (mainly repulsion) arising between ligands [5]. Note, for example, the *syn* orientation of the polycyclic aromatic hydrocarbons observed in the sandwich complexes bis(η^6-triphenylene)chromium and bis(η^6-fluoranthene)chromium [6] and bis(η^6-naphthalene)molybdenum(0), bis(η^6-1-methylnaphthalene)molybdenum(0), and bis(η^6-1,4-dimethylnaphthalene)molybdenum(0) [7]. Similarly, the *syn* conformation in bi- and trimetallic conjugated ferrocene-based complexes is preferred over the anti one [8]. Clearly, these observations cannot be explained in terms of steric repulsion between bulky ligands.

In this contribution we will concentrate on the coordinatively unsaturated two-legged piano stool complexes $Cp'ML_2$ (Cp' = cyclopentadienyl or a derivative, M = ruthenium(II) and iron(II). L = phosphorus and nitrogen co-ligands). The intriguing features of these compounds are their geometries because of the observance of both planar (pseudo-C_{2v}, i.e. the Cp' plane lies perpendicular to the L–M–L plane) as well as pyramidal structures, and thus a potential chirality at the metal. Furthermore, whereas ruthenium(II) complexes are in the majority diamagnetic, iron complexes often adopt a high spin configuration, because it costs more energy to pair electrons in the smaller Fe 3d orbitals than in the more diffuse Ru 4d orbitals. Therefore, the strong ligand-sensitivity of the spin-state of iron complexes is a welcome basis for studying 'structure–property' relationships. It is indeed highly desirable to understand in more detail the parameters that are related to stability, reactivity, structure, and spin state. This goal will be achieved by the synergistic use of theoretical and experimental data. At first we shall review the state of affairs. In the next section we occasionally include also other complexes than those specified above which are nevertheless pertinent to the issue and help one get a general overview.

2. State of affairs

The configurational stability of pyramidal ('bent') versus planar ('orthogonal', C_{2v} symmetry) 16e-complexes is traditionally treated in terms of electronic ligand effect and spin state of the metal center. A closer view reveals, however, that the whole topic is not amenable to adequate treatment by only considering these two aspects. An advancement is achieved upon adding a new perspective via the through-space coupling theory.

2.1. Electronic ligand effect

Electronic ligand effects have been analyzed with the EHMO methodology and density functional theory (DFT) by the groups around Hofmann [9], Eisenstein [10], and others. As a result, pure σ and π donors favor a planar geometry. Conversely, the possibility exists to stabilize a pyramidal geometry, at least for Cp and

benzene complexes, in the case of good π-accepting ligands, which should be good σ donors as well. Such ligands containing low-lying π-acceptor orbitals include CO, CS, and NO^+. However, there are exceptions to the rule. For example, $[CpFe(SiH_3)_2]^-$ adopts a pyramidal geometry eventhough the silyl ligand is a strong σ donor [9]. Similarly, the $\{Cp'RuCl_2\}$ fragment in the tetrameric $(Cp^*RuCl)_4$ [11] is pyramidal instead of the expected dimeric planar structure, or in the dimeric complex $[(Cp^*RuCl)_2(\mu\text{-}Cl)_2]$ [12,13] the $[CpRuCl_2]$ fragment approaches a pyramidal rather than a planar structure.

Apart from such exceptions, many complexes conform to the rule. Thus, due to σ and π donation from the trigonal planar N atom, $\{(\eta^6\text{-}p\text{-cymene})Ru(\eta^2\text{-}NH_2CHPhCHPhN(SO_2p\text{-toluene})\}$ adopts the planar geometry, [14] similar to the very recently described π-stabilized 16e-complex Cp*Ru(RNCR′NR) (R = *t*-Bu, Cy). In the latter, the amidinate ligand is acting as both a σ and π donor to compensate unsaturation [15]. This tendency of compensation is manifested in the bending of the N–C–N plane of the amidinate ligand with participation of a π-allyl N–C–N system. According to the crystal structure, the center of the Cp* ring, the Ru atom, and the two nitrogen atoms lie on the same plane, whereas a plane consisting of the Ru atom and two nitrogen atoms makes an angle of 48.9° with a plane of the amidinate N–C–N moiety [15]. A connection to the structures of the complexed polycyclic aromatic hydrocarbons mentioned in the Introduction is obvious. Slight bending is observed in $[(\eta^6\text{-}p\text{-cymene})Ru\{\eta^2\text{-}PhTAP\}]^+$ (PhTAP = $(^iPrN)_2PPh(NH^iPr)$, in which case the NH^iPr group remains uncoordinated, and the PhTAP ligand is both a σ and a π donor [16]. A comparable situation is found in various $(\eta^6\text{-arene})Ru(SAr)_2$ complexes [17].

In the course of our efforts to synthesize and characterize coordinatively unsaturated ruthenium complexes, we have recently switched over to nitrogen donors. In this way the first genuine cationic 16e-complexes $[Cp^*Ru(Me_2NCH_2CH_2NR_2)]^+$ (R = Me, *i*-Bu) [18,19] and $[CpRu(Me_2NCH_2CH_2NMe_2)]^+$ [20] became available. These nearly C_{2v} symmetric complexes are astonishingly stable, particularly those of Cp*, and show surprisingly little affinity towards the simple ligands N_2, H_2, and ethylene. This stability is the more remarkable since neither a π-donor [21] nor a bulky ligand system is involved. This phenomenon is explained in terms of the hard σ-donor character of the 'NN' ligands [15].

Related planar ruthenium compounds with phosphorus donor ligands remain unknown, in contrast to the corresponding iron analogues [22]. For the structural differences, at first glance the π-acceptor capability of PR_3 might be implicated [23], but the planar structure often found for the 16e iron congeners makes this argument contestable. While $[Ru(\eta^5\text{-ring})(PP)]^+$ ('PP' = chelate phosphorus ligands) complexes are virtually unknown, or are too reactive to be isolated, the existence of $[Cp^*Ru(PPr^i_2Me)_2]$ has been reported very recently by Puerta and coworkers [24]. The nearly planar structure found contrasts with the bent structure of the 16e-complex $[Cp^*Ru(dippe)]^+$ (dippe = $^iPr_2PCH_2CH_2P^iPr_2$). The bent geometry is explained by an agostic interaction of the hydrogen atoms of an isopropyl group with the ruthenium center, partially compensating the coordinatively unsaturated character. There is, however, no agostic interaction in the aforementioned planar $[Cp^*Ru(PPr^i_2Me)_2]^+$ complex. It has been speculated that the smaller P–Ru–P angle imposed by the chelating phosphine lowers the energy of the LUMO such that agostic donation becomes feasible [25].

In all the cases mentioned above chelate effect does not play a particular role. Half sandwich complexes with ligands of diverse nature adopt variable geometries, depending on the relative strength of ligand effects. An instructive example is found in the computational study of electronically and coordinatively unsaturated [Cp*W(NO)(L)] complexes. While with L = CO, CH_2 the pyramidal conformation is more stable, the complex with L = PH_3 is planar. In between are the weak σ-donors $H_2C{=}CH_2$ and HC≡CH, giving rise to a pyramidal geometry in the former and a planar one in the latter case [26,27].

Along these lines it is obvious that the planar structure is maintained in the unsaturated $Cp^*Ru(PR_3)X$ complexes (R = Cy, ^iPr, ^tBu, X = halide, alkoxide, amide) or Cp*Ru(carbene)X (carbene = 1,3-R_2-imidazol-2-ylidenes). According to ab initio SCF calculations [28] open-shell Ru complexes are stabilized in the presence of strong π-donor ligands X [29–38]. If the π-donor ligand X is replaced by π-accepting CO, the planar complex is destabilized and tends to add weak ligands. With such an adduct, namely the d^6 complex $(\eta^5\text{-Cp})Ru(CO)(ER_3)ONO_2$, a kinetic study has been performed of replacing the weakly coordinating nitrate with chloride [39]. Since the reaction rate was found to be independent of the chloride concentration under pseudo-first-order conditions, the transient formation of a 16e-complex is indicated. However, the increase in the first-order rate constant in the order ER_3 = $P(OPh)_3 < PPh_3 < P(p\text{-anisyl})_3 < AsPh_3 \ll PPh_2(o\text{-anisyl})$ is not in line with the expectation that a stronger donor ligand stabilizes the coordinatively unsaturated positively charged intermediate. Admittedly, the labilizing effect of PPh_2(*o*-anisyl) may be rationalized by additional coordination of the potentially chelating *o*-OMe group, but it is not clear, why $AsPh_3$ should be more effective than PPh_3. The intermediacy of a coordinatively unsaturated complex has also been considered to explain the fluxionality of the solvent L

in $[Ru(L)(N–N)(arene)][SbF_6]_2$, where N–N is bis(oxazoline) [40].

2.2. Spin state effect

Apart from the electronic properties of the ligands their steric properties also have to be considered as well as the spin state of the metal. From studies on iron(II) half-sandwich complexes it has been claimed that the orthogonal and bent structures, respectively, adopt $S = 1$ and $S = 0$ spin configurations [22]. Likewise, the aforementioned 16-electron triplet [CpW(NO)(L)] species have a planar conformation, whereas the singlet state is highly pyramidal. This feature is rationalized in terms of the ratio of the frontier orbital energies of the complexes. The presence of both pure σ and π donor ligands in the dimer of iron(II) halides $[(Cp')FeBr]_2$ ($Cp' =$ tetra and penta isopropylcyclopentadienyde) change the orbital energies so greatly that the complex has maximum spin with four uncoupled electrons [41]. Contrary to expectation, however, the neutral half-sandwich complex $FeCp^*[N(SiMe_3)_2]$ is diamagnetic, albeit trigonal planar N atom is both a good π- and σ-donor [42]. The solid state structure of this diamagnetic complex is unprecedented in open shell organometallic chemistry.

For complexes having good σ- donor and weak π-acceptor phosphine ligands, the triplet state is the ground state. Hitherto five unsaturated complexes of the type $[Fe(\eta^5\text{-ring})(PP)]^+$ (ring = Cp, Cp*, pentadienyl; 'PP' = $Ph_2PCH_2CH_2PPh_2$ (dppe), $Pr^i_2PCH_2CH_2P$-Pr^i_2P (dippe), $2\cdot PEt_3$) have been isolated and structurally characterized [43–45]. All of them have planar ground state structures and are paramagnetic ($S = 1$). These results have been nicely reproduced by DFT calculations by Costuas and Saillard [22] in terms of both a small HOMO–LUMO gap and weak HOMO–LUMO overlap (rendering the Jahn–Teller instability of the pseudo-C_{2v} geometry insignificant). Noteworthy, if a singlet ground state is assumed, the pyramidal structure is favored. Thus, the relative stability of the iron complexes under consideration can be traced to the energetically unfavorable change in spin state preventing the unsaturated complex from adding nucleophiles. This point of view has been put forward by Poli [3]. For certain ratios of electron pairing energy to HOMO–LUMO gap, the paramagnetic nature is retained on going from planar $[Cp^*Fe(LL)]^+$ to the 18e adduct in which the {Cp*Fe(LL)} fragment has a pyramidal conformation. For instance, the 18e complexes $[Cp^*Fe(AN)(dippe)]^+$ and $[Cp^*Fe(Me_2CO)(dppe)]^+$ are paramagnetic, whereas the $[CpFe(AN)(dippe)]^+$, $[CpFe(AN)(dppe)]^+$, and $[Cp^*Fe(AN)(dppe)]^+$ analogues are diamagnetic [44]. Consequently, it is not possible to definitely predict the structure of the iron(II) complexes solely from the spin state.

It is quite common for organometallic compounds in general that increasing covalency enhances the energy gap between the strongly anti-bonding and the non bonding (or weakly anti-bonding) orbitals. This gap is increased as we move down the series from 3d to 5d. In other words, the 4d and 5d transition metals form stronger bonds than their 3d congeners [4] in which case the electron pairing energy is much lower than the HOMO–LUMO gap, and the low spin state is preferred. In fact, stable high-spin d^6 ruthenium half-sandwich 16e-complexes are actually unknown. However, it is wrong to state that singlet-triplet crossing does not occur in half-sandwich Ru complexes. The formation of a high-spin compound from $Ru(\eta^6\text{-arene})(L)_3^{2+}$ occurs by ultraviolet irradiation noting triplet lifetimes of < 10 ns [46]. As it is known, $Cp'RuCl(PPh_3)_2$ ($Cp' =$ indenyl, Cp) induces radical polymerization [47]. Since the latter is a spin forbidden process, it is reasonable to speculate that it is effected through the intermediacy of a high-spin half sandwich complex. By and large, however, spin state arguments are less relevant to structural considerations of the stabilization ruthenium complexes.

In summing up the results, the factors that determine the structure of the 16e two-legged piano stool complexes and the mechanism of the planar/pyramidal structure rearrangement are not fully understood. Clearly, the interpretation solely in terms of electronic ligand effects and spin-state effects is not the whole story. Sometimes the deviations from expected structures can be reproduced by analyzing calculated orbital and total energies. Notwithstanding this the underlying physical reasons remain hidden. Hitherto explanations for all of the exceptions to the spin state or the electronic ligand effect rule try to use stand-alone assumptions without a subordinate concept.

2.3. The through-space coupling (TSC) concept

In the following we shall show that the implication of interligand interactions by means of the TSC concept definitely advances the topic. Note that the present paper is a continuation of our former work in which we successfully applied the TSC concept to rationalize the diverse array of structural arrangements as well as reactivities of the main-group Cp metal complexes [48]. The basic idea of the TSC concept is that in a metal complex the ligands approach so closely to one another that their orbitals interact with each other. When, for example, two localized orbitals (φ, vacant or φ*, filled) interact, two pairs of new collective orbitals, combined by sum and difference, are formed: the symmetric (in-phase) orbitals $1\Psi_s^{TSC}$ and $2\Psi_s^{TSC}$ (bonding orbitals) and the higher energy, anti-symmetric (out-of-phase) orbitals $1\Psi_a^{TSC}$ and $2\Psi_a^{TSC}$ (antibonding orbitals) (Scheme 1). This aspect calls to one's mind a formal fragment orbital analysis. The energy splitting

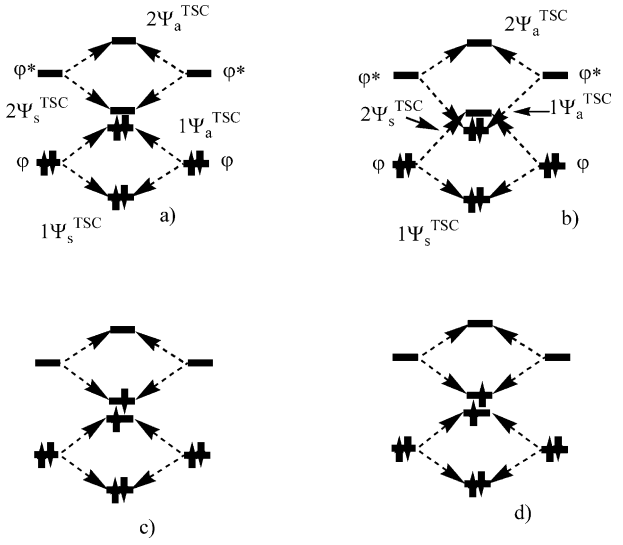

Scheme 1.

between the two orbitals is a quantitative measure of orbital interaction. If both orbitals are doubly occupied, there is indeed overall loss in energy corresponding to van der Waals (vdW) repulsion (case a). This is a manifestation of covalent antibonding. But electron density can be removed from the antibonding TSC orbital into some vacant orbital either of the ligands themselves (for example, TSC orbital formed as in-phase combination of the antibonding orbitals of the separate participants—case b), or of the coordination center (AO's of metal). In this way electron–electron repulsion is minimized and the molecular construction acquires additional stability through vdW attraction.

Case a represents the basic principle of intramolecular singlet or triplet excimer formation (cases c and d) such as the lowest, triplet Σ excited states of He_2^*, namely the $a(^3\Sigma_u)$ and $c(^3\Sigma_g)$ states with electron configurations $1\sigma_g^2\ 1\sigma_u\ 2\sigma_g$ and $1\sigma_g^2\ 1\sigma_u\ 2\sigma_u$ at equilibrium [49] or other metastable rare gas excimers [50,51]. Of course more electron rich aromatic compounds form much more stable excimers as found with α,α-dinaphthylalkanes [52] and naphthalenophanes [53] with a preferred overlapping sandwich configuration. It is π–π interactions between polycyclic arenes in the excited singlet and triplet states that effect a fully eclipsed parallel orientation [54]. If the symmetric TSC orbital $2\Psi_s^{TSC}$, formed from the antibonding orbitals of the separate participants, is lower in energy than $1\Psi_a^{TSC}$ (case b), vdW attractive forces come into play. For example, supramolecular coordination polymeric architectures are formed like the double-decker silver(I) coordination polymer with columnar aromatic stacks [55]. Further, decreased repulsive π-interactions between benzene rings are clearly obvious since the interannular distances between two decks of [2.2]paracyclophane (pcp) in the mononuclear complexes of Rh and Ir, $[Cp^*M(\eta^6\text{-pcp})](BF_4)_2$ are shorter than that of the metal-free pcp ligand [56]. Such novel transition metal complexes of cyclophanes continue to be an exciting area of organometallic chemistry.

It is commonly thought that interligand interactions are always repulsive in nature and represent a minor component of the global energetic balance, while M–L bond formation energies dominate the situation. But this is a superficial point of view. Because of the short distances between the coordinated ligands, their orbitals can interact with each other according to Scheme 1. In this case the donor ability of a pair ligands, determined by the $1\Psi_a^{TSC}$ orbital, can even be increased relative to the separate φ orbitals with the M–L bond strengthened. Powerful interligand interactions (repulsive and attractive) are one of the reasons why any attempts to estimate separate metal–ligand bond strengths have been unsuccessful.

In applying the TSC concept to complexes of the type $Cp'ML_2$, the individual lone pair orbitals of the L_2 ligand give the TSC orbitals Ψ_a^{TSC} (out of phase) and Ψ_s^{TSC} (in phase). These are then linearly combined with both the symmetric (a'_2) and antisymmetric (e'_2) orbitals of Cp yielding a second generation of TSC orbitals (Ψ_{ss}^{TSC}, Ψ_{as}^{TSC} and Ψ_{sa}^{TSC}, Ψ_{aa}^{TSC}, vide infra). Since all orbitals are filled, the bonding orbitals Ψ_{ss}^{TSC}, Ψ_{sa}^{TSC} determine the interligand vdW attraction, while the antibonding orbitals Ψ_{as}^{TSC}, Ψ_{aa}^{TSC} are responsible for vdW repulsion between Cp′ and the L_2 group. On the one hand, the interactions of these four TSC orbitals with the metal AO's are more effective than the interactions of the separate ligand orbitals, because of better overlap. On the other hand, the shift of electron density from the antibonding TSC orbitals, especially from Ψ_{aa}^{TSC}, is decisive for the stability of the metal complex topology minimizing interligand repulsion.

3. Results and discussion

3.1. The geometry of $Cp'ML_2$ complexes

At first we present the results of our analysis of the CpRu(PP) and CpRu(NN) complexes based upon DFT calculations. The intention is to compare the electronic structures of coordinatively unsaturated half sandwich iron and ruthenium complexes, using N and P donor coligands, as well as their reactivities towards simple donor ligands like N_2,H_2, O_2, and others. To reduce computational effort, $[Cp^*Ru(Me_2NCH_2CH_2NMe_2)]^+$ and the analogous bisphosphine complex have been modeled by the smaller species $[CpRu(NH_3)_2]^+$, $[CpRu(H_2NCH_2\text{-}CH_2NH_2)]^+$, $[CpRu(PH_3)_2]^+$, and $[CpRu(H_2PCH_2\text{-}CH_2PH_2)]^+$. The major results of the DFT-optimized geometries of these complexes as well as the structural data of $[Cp^*Ru(Me_2NCH_2CH_2NR_2)]^+$ (R = Me, *i*-Bu)

Table 1
Experimental and optimized structural data for various $[RuCpL_2]^+$ complexes

$[RuCpL_2]^+$	M–L (Å)	M–C_5 av (Å)	L–M–L (°)	α (°)[a]
$[RuCp(H_2NCH_2CH_2NH_2)]^+$	2.218	2.165	78	171
$[RuCp(NH_3)_2]^+$	2.202, 2.192	2.196	91	179
$[RuCp(Me_2NCH_2CH_2NMe_2)]^+$	2.142(6), 2.163(8)	2.09(1)	80.9(1)	180
$[RuCp^*(Me_2NCH_2CH_2Nme_2)]^+$	2.183(7), 2.180(6)	2.142(7)	80.3(3)	179
$[RuCp^*(Me_2NCH_2CH_2N(i\text{-}Bu)_2)]^+$	2.18(1), 2.21(1)	2.13(1)	78.1(5)	168
$[RuCp(H_2PCH_2CH_2PH_2)]^+$	2.346	2.248	83	149
$[RuCp(PH_3)_2]^+$	2.356	2.241	96	152
$[RuCp^*(PmePr^i_2)_2]^+$	2.393(1), 2.395(1)	2.182(5)	101.4(1)	171
$[RuCp^*(dippe)]^+$	2.331(1)	2.207(5)	83.1(1)	169

[a] α = Cp(centroid)–Ru-L_2 (centroid).

and $[CpRu(Me_2NCH_2CH_2NMe_2)]$ [18–20] are presented in Table 1. Relative B3LYP energies of optimized structures of $[CpRu(H_2NCH_2CH_2NH_2)]^+$ and $[CpRu(H_2PCH_2CH_2PH_2)]^+$ at various angles α = Cp(centroid)–Ru–L_2 (centroid) are sketched in Fig. 1. While the potential energy surface for the inversion of the amine complex is very flat, for the phosphine complex there is an energy difference of about 6 kcal mol^{-1} between an ideally planar (180°) and a pyramidal (149°) geometry. The ground state structure of the amine complex adopts a pseudo-C_{2v} structure, and the phosphine complex is strongly pyramidalized with α = 149°. The optimized geometry of $[CpRu(H_2NCH_2CH_2NH_2)]^+$ is close to the experimental structure of $[Cp^*Ru(Me_2NCH_2CH_2NR_2)]^+$ (R = Me, *i*-Bu) and $[CpRu(Me_2NCH_2CH_2NMe_2)]$ for which α varies between 168 and 180° (Table 1). Bending of the C_{2v} symmetric $[CpRu(H_2NCH_2CH_2NH_2)]^+$ by α = 30° is calculated to require only about 2.2 kcal mol^{-1}. In view of such a low barrier, the variation of the experimental α values is not unexpected.

The differences in the degree of bending in the CpRu(PP) and CpRu(NN) complexes as suggested from DFT are similar to those described for the diamagnetic iron analogues [9] and further are in accord with a recent EH analysis [19]. However, the actual reason for the divergent bending tendencies remains vague, but is illuminated in the TSC picture which emphasizes the involvement of in-phase and out-of-phase combinations of the lone pairs of the P or N atoms represented by the TSC orbitals Ψ_s^{TSC} and Ψ_a^{TSC}. It is well known that in the absence of d orbitals, the Cp–M bonds are longer than those in the transition metal complexes [57]. This occurs on the grounds of symmetry since the antibonding orbitals (Ψ_{aa}^{TSC}) cannot interact with the (main-group) metal AO's. The underlying effects are dramatic as can be delineated from the linear relationship between the metal–Cp distances in alkaline-earth-metal complexes and the metal radii as elaborated by Sockwell and Hanusa [58]. These data would predict C(Cp)–Fe and C(Cp)–Ru distances of 2.57 and 2.65 Å, respectively, compared to the actual values of 2.02–2.10 Å for Fe, and 2.19–2.20 Å for Ru [59]. The decrease in distance reflects the partial removal of vdW repulsion between the ligands by electron density shift from the filled antibonding TSC orbitals. If this is not feasible as in the case of the d^{10} complexes like Zn(II) [9], the antibonding TSC orbitals provoke a

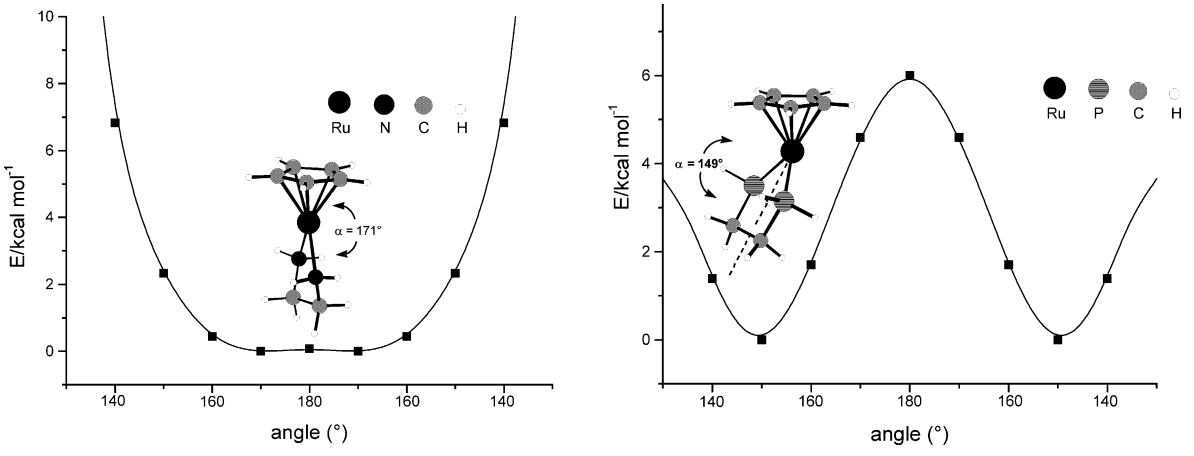

Fig. 1. B3LYP energies of optimized $[CpRu(H_2NCH_2CH_2NH_2)]^+$ and $[CpRu(H_2PCH_2CH_2PH_2)]^+$ at various angles α = Cp(centroid)–Ru–L_2(centroid).

conformational flexibility found in zirconocene $[(C_3H_7)_4C_5H]_2Zn$, which has a slipped-sandwich structure [60] similarly to the alkaline-earth metallocenes [48].

The TSC orbitals have either more Cp′ or L_2 character, depending on the energy levels in accordance with the values of the overlap populations (OV POPs). The individuality of the TSC orbitals of the 'NN' ligands is more pronounced than those of 'PP', because the 3s, 3p AO's of the P atom are more spaciously diffuse than are the 2s, 2p AO's of the N atom. Since, further, the distances between the Cp plane and the N and P atoms are very similar (Table 1), stronger mixing of the TSC orbitals can be expected for the 'PP' complexes. This reasoning is corroborated by calculations on the EH-level: the OV POP's in the Cp–'PP' system are noticeably larger, reaching values of 0.01–0.05 compared to <0.01 for Cp–'NN'. This feature has a bearing on the geometry.

Table 2
Overlap population analysis (EH level) for the main interactions in the CpRu(PP) and CpRu(NN) complexes based on the DFT optimized structures

Interaction	$CpRu(H_2PCH_2$-$CH_2PH_2)$		$CpRu(H_2NCH_2$-$CH_2NH_2)$	
	Planar	Pyramidal	Planar	Pyramidal
$<\Psi_{aa}^{TSC}\|d_{xz}>$	0.38	0.44	0.21	0.16
$<\Psi_{sa}^{TSC}\|p_x>$	0.36	0.38	0.12	0.13
$<b_1\|d_{yz}>$	0.30	0.17	0.25	0.11
$<\Psi_{as}^{TSC}\|p_z>$	0.11	0.12	0.10	0.08
$<\Psi_{ss}^{TSC}\|s>$	0.19	0.21	0.10	0.08
TSC splitting (ΔE eV)[a]	0.21	0.41	0.023	0.053

[a] The total energy loss upon the interaction of Cp and 'PP' or 'NN' ligands for the different complex geometries.

In the planar half-sandwich complexes, the $Cp'L_2$ ligands have virtually only five orbitals capable of

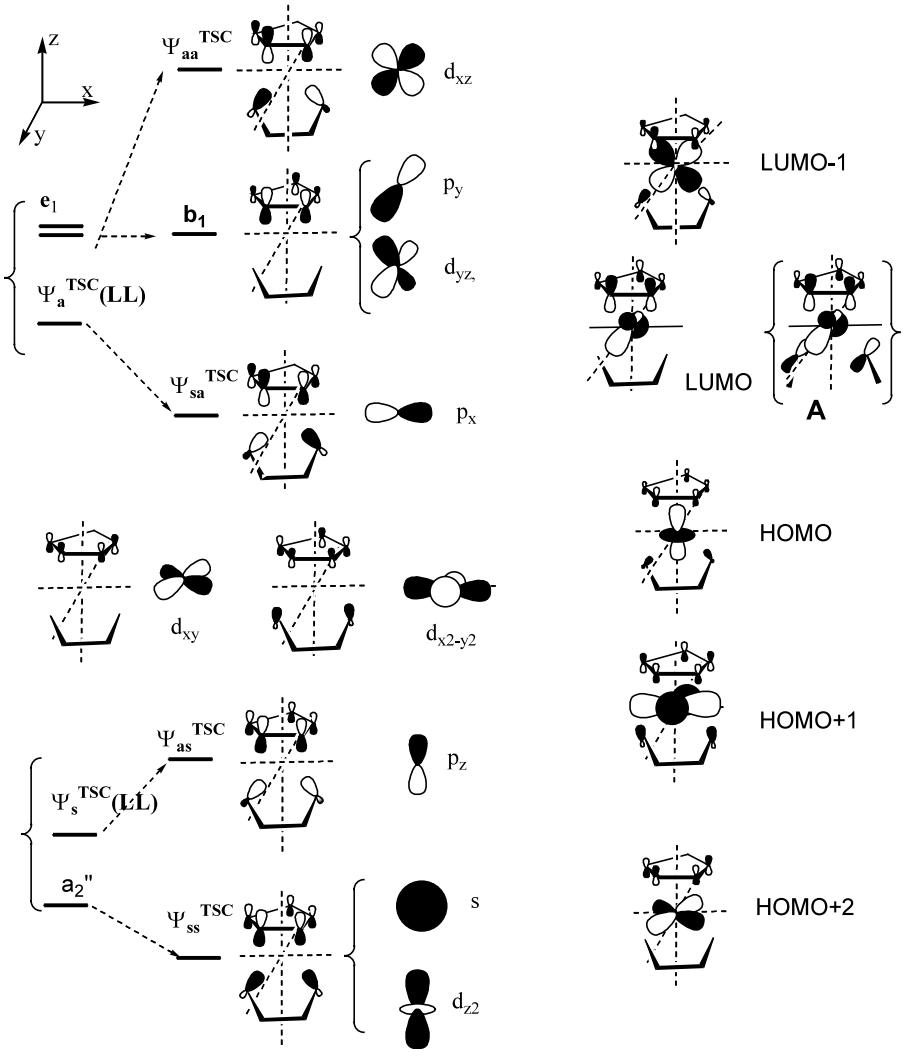

Fig. 2. Planar $CpML_2$. The formation of relevant TSC orbitals of the ligand system {Cp, L–L} from separate orbitals of Cp (a'_2, e1) and L_2 (Ψ_a^{TSC}, Ψ_s^{TSC}) (left side). Suitable metal AO's for the interaction are shown in the middle. The active orbitals derived from these interactions are shown at the right side. (A) Stabilizing effect of the filled π orbitals of L,L ligands.

interaction with the metal AO's, namely four TSC orbitals (Ψ_{ss}^{TSC}, Ψ_{as}^{TSC} and Ψ_{sa}^{TSC}, Ψ_{aa}^{TSC}) and one of the e_1 orbitals of Cp′ (b_1) (Fig. 2, left). These orbitals can interact with the symmetrically suitable metal AO's with overlap populations displayed in Table 2. Most important is the filled antibonding obital Ψ_{aa}^{TSC}, which is high-lying (1.24 eV, according to DFT calculations) and largely responsible for the interligand vdW repulsion. DFT calculations on the Cp–'NN' system using the optimized geometry of the CpRu(NN) complex shows some negative vibrational frequencies anticipating the movement of the Cp and 'NN' ligands so as to minimize the orbital interactions in Ψ_{aa}^{TSC}. The actual extent of the repulsions is recognized by the total TSC splitting energy (ΔE) (Table 2). Now, due to the $\langle \Psi_{aa}^{TSC} | d_{xz} \rangle$ interaction (Fig. 2.), electron density is withdrawn from Ψ_{aa}^{TSC} partially converting the interligand vdW repulsion into vdW attractions.

Important orbitals for planar $Cp'ML_2$ are depicted in Fig. 2. Three metal orbitals, viz. d_{z2}, d_{xy} and d_{x2-y2}, are rather nonbonding, since the filled-filled $\langle \Psi_{ss}^{TSC}(LL) | d_{z2} \rangle$ and $\langle \Psi_{s}^{TSC}(LL) | d_{x2-z2} \rangle$ orbital interactions are weak and push up the d_{z2} and d_{x2-y2} orbitals only slightly, whereas the empty-filled $\langle e_1^* | d_{xy} \rangle$ and $\langle e_1^* | d_{x2-y2} \rangle$ orbital interactions slightly push down d_{xy} and d_{x2-y2}, forming the HOMO, HOMO+1 and HOMO+2.

Thus, the HOMOs are metal-like in character. The LUMO of the complex, on the other hand, derives from the antibonding part of the $\langle b_1 | d_{yz} \rangle$ interaction which is enhanced through the participation of the vacant metal p_y orbital. Since the orbitals of L_2 are not particularly involved, the HOMO–LUMO gap in $Cp'ML_2$ is determined by the nature of the metal rather than the ligands. In view of the lower electron affinity of Fe^{2+} compared to Ru^{2+} (16.18 vs. 16.76 eV) [61] the e1 orbitals of the Cp unit interact less strongly with the d_{xz} or d_{yz} AO's of the former. Consequently, the gap is smaller for the iron complexes (which therefore are often paramagnetic) and increases in going from the 3d to the 4d metals.

From the present analysis it is concluded that the planar $CpML_2$ complexes are relatively stable and unreactive, because of the unsuitable orientation of the frontier or, better, active orbitals. Thus the low-lying vacant orbital (where the entering ligand has to attack) and the donor orbital both are arranged parallel to Cp plane. Consequently, the activation step has to involve bending towards a pyramidal structure to direct the vacant orbitals towards the free space. It is important to emphasize that such bending does not deteriorate, but to the contrary may even slightly strengthen the interactions (between Ψ_{ss}^{TSC}, Ψ_{as}^{TSC} and Ψ_{sa}^{TSC}, Ψ_{aa}^{TSC} and the metal AO) that are responsible for the complex stability. This feature is visualized in Fig. 3 and recognized by the values of the overlap population presented in Table 2.

The driving force for the planar/pyramidal inversion involves strengthening of the interactions between the metal AO's and the TSC ligands orbitals via the orbitals Ψ_{as}^{TSC} and Ψ_{aa}^{TSC}, depending on the nature of L_2. Since, of course, nitrogen has smaller orbital radii and less diffuse orbitals than phosphorus, the TSC interaction is more efficient for the latter. This is reflected by the TSC splitting energy ΔE^{TSC} which is virtually meagre for the Cp–'NN' system (Table 2). Similarly, the increase in ΔE^{TSC} upon bending is more remarkable for the Cp–'PP' system. Actually, the stronger mixing of the TSC orbitals renders an additional stability of the complex. The more efficient involvement of the 'PP' ligand orbitals is also established by the DFT analysis above. Thus, the participation of the amine ligands in both the HOMO and the LUMO of $[RuCp(H_2NCH_2\text{-}CH_2NH_2)]^+$ and $[RuCp(NH_3)_2]^+$ is rather weak, but is increased upon switching over to the P congeners. Since, furthermore, the participation of the 'PP' ligand orbitals is slightly more pronounced on bending, the phosphorus complexes are pyramidal in the ground state, whereas the potential energy surface for the inversion of the amine complex is very flat.

Such a stabilization of the pyramidal construction should also be expected for the 16e iron complexes such as $[FeCp(PP)]^+$. The gain in energy by TSC, however, is counterbalanced by two other effects, namely the excessively low-lying LUMO, whose energy is determined primarily by the iron d_{yz} orbital, and secondly by the uncoupled electron collapse energy (from $S=1$ to $S=0$). As a result, the energy difference between the planar triplet state and the pyramidal singlet state of 'PP' complexes is negligible, lying in the range of 0.01–0.14 eV [22]. On the other hand, the absence of the stabilization by TSC in the 'NN' iron complexes, independent of geometry, makes complexes such as $[Cp^*Fe(tmeda)]^+$ actually unstable.

It should further be noted that bending gives rise to several additional TSC orbital interactions capable of changing stability and reactivity. Of these interactions, three variants are particularly relevant: (i) the strengthening of the $\langle b_1 | d_{yz} \rangle$ interaction through the formation of a new TSC orbital between b_1 and Ψ_{ss}^{TSC} of the L_2 group (Fig. 3, A) results in a high-lying LUMO of the bent complex that is optimally oriented for nucleophilic attack to occur. This contrasts sharply with the low-lying LUMO in the planar construction. (ii) π-Acceptor ligands can appreciably relax the destabilizing effect of the $\langle \Psi_{ss}^{TSC} | d_{x2} \rangle$ interaction (Fig. 3D) via back-bonding, i.e. electron density shift from the metal into the π*-acceptor orbital (M→L shift). Clearly, π-donor ligands have the opposite effect and thus favor a planar geometry (see also Figure 4 of Ref. [9]). (iii) While in the planar system the metal d_{xy} AO is virtually nonbonding, upon bending a new interaction arises between it and Ψ_{a}^{TSC} of the L_2 group with participation

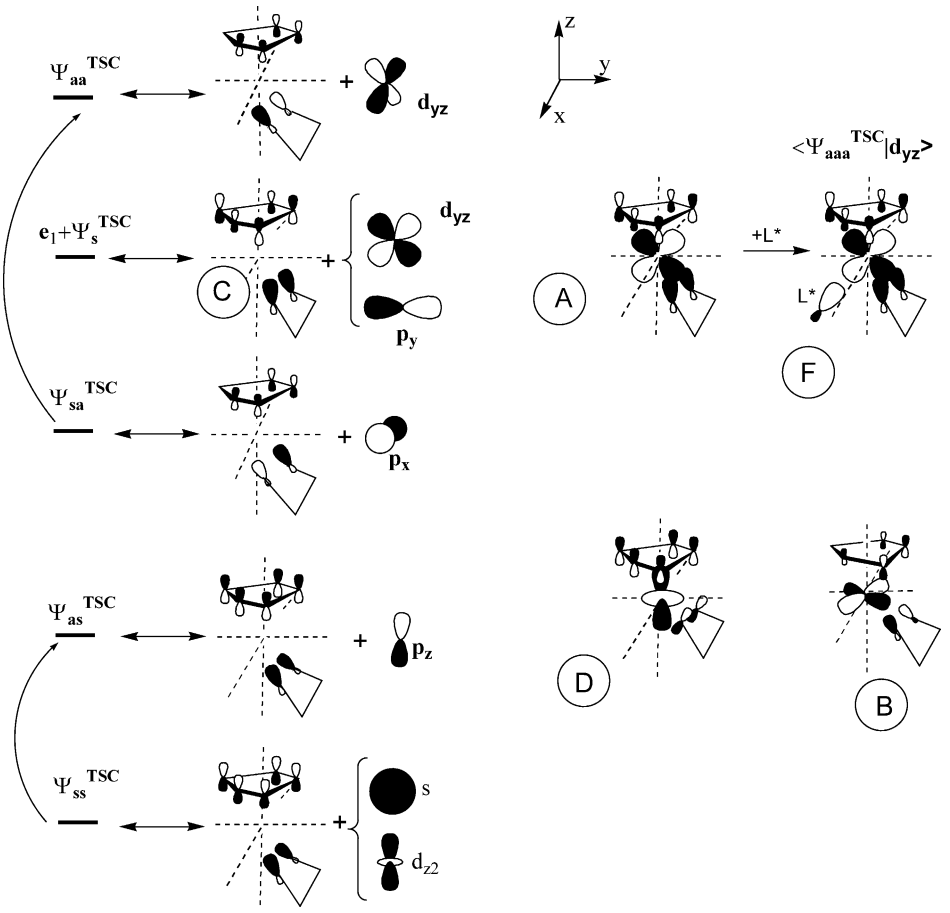

Fig. 3. Variation of the TSC orbitals from Fig. 2 upon bending (left side). Suitable metal AO's for the interaction are shown in the middle. Particular results: (A) strengthening of the $\langle b_1|d_{yz}\rangle$ interaction (formerly LUMO); (B) new interaction with the metal d_{xy} AO upon bending (formerly HOMO+2); (C) distorted TSC orbital (formerly b_1); (D) relaxed destabilizing effect of the $\langle\Psi_{ss}^{TSC}|d_{z2}\rangle$ interaction by a π-acceptor ligand orbital; (F) formation of a closed TSC orbital by the attack of a third ligand L*.

of the strongly antibonding π* orbital of Cp (Fig. 3B). In this way the energy and orientation of HOMO can change. Albeit the perturbation of the metal d(σ) AO's does not affect the HOMO/LUMO gap, the HOMO alters its orientation and hence the donor property of the complex.

Along these lines the TSC concept provides a framework which allows one to rationalize hitherto unexplained observations and to understand the underlying reasons. Evidently, pure hard σ-ligands have weak TSC interactions with the Cp system and therefore can destabilize the bent structure and hence favor the planar geometry. As an example, the pyramidal geometry of bent $[CpFe(H_2)]^-$ is computed to be only 0.94 kcal mol^{-1} (0.04 eV) more stable than the planar one. Furthermore, energy barriers for distortion are extremely shallow [9]. Soft σ-ligands, on the other hand, (with softness increasing in going to more electron rich elements along the series N→P→As→Sb) can effectively interact with b_1 of Cp. The resulting distorted TSC orbital C, shown in Fig. 3, can in turn better interact with the metal d_{yz} orbital. Hence the bent conformation is favored. From this point of view it is understandable that the pyramidal geometry of $[CpFe(SiH_3)_2]^-$ is not the result of the strong electropositive σ-ligands, but rather the strong TSC interaction between the two silyl ligands. This effects powerful TSC splitting $\Psi_a^{TSC}/\Psi_s^{TSC}$ as high as 2.9 eV [9] comparable with the 3.0 eV calculated for the chelate 'PP' ligand $Me_2PC_2H_4PMe_2$ [19]. Also, the mixing between Ψ_a^{TSC} and e1 of Cp is enhanced. Analogously, the stabilizing effect of $AsPh_3$ relative to PPh_3 in (η^5-Cp)Ru(CO)(ER_3) noted above [39] is due to the stronger TSC interaction between e1 of Cp and 4s,p AO's of As which are more diffuse than the 3s,p AO's of P. Likewise, the TSC interaction between Cp′ and tris Cl ligands behind the metal center in tetrameric {(Cp′RuCl)$_4$} is more powerful in the octahedral surrounding in the {Cp′$RuCl_3$} fragment [11] than in the expected planar dimer construction. In the absence of the $\langle\Psi_{aa}^{TSC}|d_{xz}\rangle$ interaction as in the case of the aluminum complex $[CpAlCl_3]^-$, interligand vdW repulsion due to the high-lying filled Ψ_{aa}^{TSC} orbital provokes Cp ring slippage along the Cl_3^- plane [62,48].

3.2. General abilities of the Cp′ML$_2$ complexes

3.2.1. The acceptor properties

Clearly, the reactivity of the unsaturated CpML$_2$ complexes is above all determined by their acceptor properties, which in turn depend on the level and the spatial orientation of the vacant orbitals LUMO and LUMO-1 (Fig. 2, right). The other vacant orbitals are too high in energy for nucleophilic attack to be feasible. Since LUMO-1 is screened, especially in the planar complex, the actually active orbital is LUMO, which, however, is situated parallel to the Cp plane and therefore has an unsuitable spatial orientation. Therefore, these C_{2v}-symmetric complexes are poor Lewis acids, being reluctant to undergo reactions with simple donor ligands. The availability of the σ-acceptor orbital of the complex is increased by the participation of the metal p$_y$ AO (Fig. 2, right). A Lewis-acidic propensity is reflected by the agostic interaction between the hydrogen atoms of an *iso*-Pr group and ruthenium in [Cp*Ru(dippe)]$^+$ [25]. Similarly, Cp*Ru(PR$_3$)(OCH$_2$R′) has been reported to form unstable Cp*Ru(H)(PR$_3$)(OCHR′) via β-hydrogen migration [10]. Also, the catalytic action of Cp*Ru-1,2-diamine complexes in the hydrogenation of ketones is interpreted in terms of Lewis acidity [63].

Even with LUMO half-occupied, the planar paramagnetic [Cp*Fe(dppe)]$^+$ 16e-complex (3.3 μ_B) is claimed to be a strong Lewis acid [43]. By a one-electron reduction, transformation takes place into the thermally stable d^7 Fe(I) Cp*Fe(dppe) whose geometry is inbetween a C_{2v} pyramidal structure with a vacant site and a distorted C_{2v} planar polyhedron [43]. Ultimately, occupation of LUMO with two electrons leads to an 18e complex without much effect on the complex construction. In this respect the complexes [Ru(Cp*)(tmbp)][Na(DME)$_2$] and [Fe(Cp*)(dppe)][MgBr·3THF] may be noted, in which the cationic fragments actually feature a leg in a distorted three-legged piano stool structure. Since the metal–metal distances exceed the sum of the covalent radii, and further the metal–Cp* centroid axes are nearly in-plane ($\alpha = 170^\circ$ for the Ru complex), the anionic fragment can alternatively be described as a two-legged piano stool. While two legged piano stool iron(0) anionic complexes are well-known for a long time, e.g. [Cp*Fe(dppe)]$^-$ [64] ([Fe(Cp or Cp*)L$_2$], L = CO [65–67], ethylene [68] or L$_2$ = diene [11], only very recently a ruthenium counterpart, viz. the thermally stable ([Ru(Cp*)(tmbp)][Na(DME)$_2$] (tmbp = 4,4′,5,5′-tetramethyl-2,2′-biphosphine) has been reported [69]. The reason for the difference in stability can be traced to the action of the antibonding part of the $\langle b_1|d_{yz}\rangle$ interaction, which increases in going from the 3d to the 4d metals. This has been discussed above in connection with the LUMO of the 16e Cp′ML$_2$ complexes (which is the HOMO of the present 18e con-

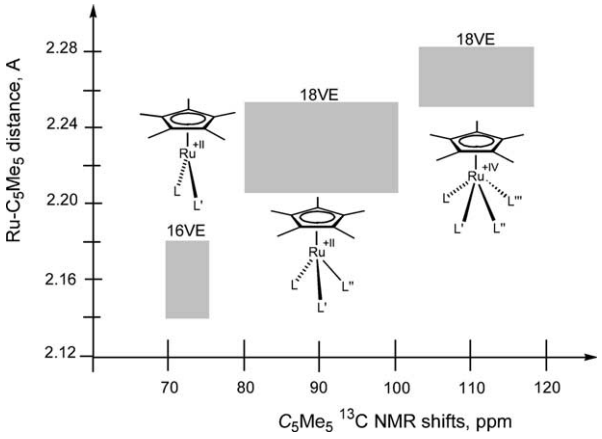

Fig. 4. Relationship between Ru–Cp* bond distances and ^{13}C-NMR resonances of the ring carbon atoms of the Cp* ligand in Cp*RuL$_n$ complexes.

geners). The filling of both parts—bonding and antibonding—of the TSC orbitals $\langle b_1|d_{yz}\rangle$ creates an additional vdW repulsion which is reflected by the increase in the Cp–metal distances. For example, the average C(Cp)–Ru(0) distance in ([Ru(Cp*)(tmbp)][Na(DME)$_2$] of 2.19 Å is close to that in the Ru(II) 18e complexes. The lengthening of the Cp–Ru distance is manifested in the ^{13}C-NMR resonances of the ring carbon atoms of Cp*. In fact, the Ru–C$_5$ distances as well as the ^{13}C-NMR resonances of the ring carbon atoms of the Cp* ligand can be used as straightforward criteria to distinguish between 16e and 18e complexes. This can be seen by the graph in Fig. 4.

3.2.2. The donor properties

While there is only one orbital relevant for the acceptor property, for the donor properties there are in principle three filled orbitals available. In the case of

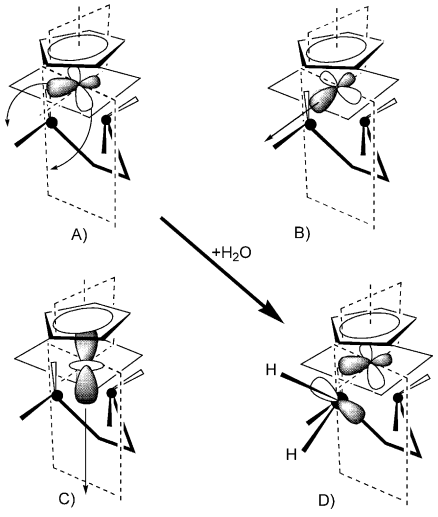

Fig. 5. 'Active' donor orbitals in bent CpM(L$_2$). (A) π donor orbital, (B, C) σ donor orbitals. (D) Destabilizing effect of the p-orbital of H$_2$O due to filled–filled interactions (vdW repulsion).

planar unsaturated Cp′ML_2, the filled d metal orbitals either remain as virtually nonbonding d_{xy} or are slightly antibonding because of the weak filled–filled $\langle\Psi_{ss}^{TSC}(LL)|d_{z2}\rangle$ and $\langle\Psi_{s}^{TSC}(LL)|d_{x2-y2}\rangle$ interactions, forming HOMO and HOMO+1 (see Fig. 2, right). The particular situation here is that all of these orbitals are high-lying, degenerate, and metal-like in character. On account of the weak interactions with Cp and L_2, the attacking ligand can upset the orbital energy ordering and act as either π or σ donor (Fig. 5A–C). For example, good π acceptors are tightly coordinated to Cp*Ru(amidinate), which therefore is a donor [15]. This feature gives rise to largely variable geometries of the resulting 18e complexes as follows. The short Ru–Si and long Si–Cl distances in $Cp(PMe_3)_2RuSiCl_3$ point to a π-interaction between ruthenium and the trichlorosilyl group, resulting from d(Ru)→σ*(Si–Cl) π-back-bonding interactions between the filled HOMO and HOMO+1 orbitals of the ruthenium moiety and the empty σ* orbitals of the Si–Cl bonds [70]. The effect of back-donation is obvious not only from the bond distances but also from the geometries. Thus the twisted (Cp(centroid)–Ru–Si–X dihedral angle ≠0) structure of $CpL_2Ru{=}SiX_2^+$ (L = PH_3, PMe_3, CO, X = H, Me, SH) reflects the participation of different donor metal d orbitals with the vacant p orbital of the Si atom [71]. The cooperation of both aspects (bond distance and geometry) is evident in the various structures (linear and nonlinear) of *para*-functionalized $[(\eta^2\text{-dppe})(\eta^5\text{-}C_5Me_5)Fe(C{\equiv}CC_6H_4X)]$ (X = NO_2, CN, CF_3, F, Br, H, Me, ^{t}Bu, OMe, NH_2, NMe_2), in which a one-electron transfer M→L on the alkynyl fragment forms metal cumulenic structures with the Fe=C=C piece [72]. The ambiguity between donor and acceptor capabilities is displayed in the reaction of the electron-rich cations $[Cp^*Ru(PMe_3)_2(SO)]^+$ and $[Cp^*Fe(PMe_3)_2(SO)]^+$ [73] whose coordinated SO is attacked by either nucleophilic 3-chloroperbenzoic acid or electrophilic pyridine and PMe_3. Notwithstanding this, from the energetic point of view, the 16e $[CpML_2]^+$ complexes may be classified as acceptors rather than donors. Conversion to anionic 18e $[CpML_2]^-$ creates a high-lying HOMO. For example, the anionic Ru(0) complex $[Ru(Cp^*)(tmbp)]^-$ is trapped with MeI, Ph_3SnCl, Me_3SnCl, or H^+ via an oxidative addition that leads to the formation of Ru(II) [69].

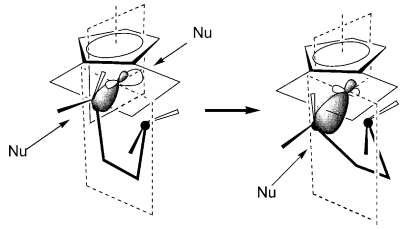

Fig. 6. Changes of the 'active' acceptor orbitals of $CpM(L_2)$ upon bending. Note the favorable nucleophilic attack in the bent complex.

Summed up, activation of the 16e planar $CpML_2$ complexes needs bending to a pyramidal structure so as to uncover the vacant orbital (Fig. 6). The small energy difference between the planar and pyramidal geometry can be easily overcome under experimental conditions. Clearly, bulky L_2 ligands hamper the bending and in this way modify the reactivity [74]. The presence of σ ligands with additional π-donor properties in RuCp*-(P^iRr_2Ph)X (X = Cl, Br, I, OCH_2CF_3, $OSiMe_2Ph$, NHPh) [10] raises the LUMO (Fig. 2A) and thus disfavors pyramidalization. Such ligands accelerate the exchange between free and bound phosphines in the 18e $Cp^*Ru(PMe_3)_2X$ complex, which proceeds by an S_N1 mechanism via an unsaturated 16e intermediate. In similar terms the *cis*-labilizing effect may be rationalized [75]. The motive force of the attack of a third ligand L* at $[Cp'ML_2]^+$ is the gain in vdW attractive energy within the {Cp′L_2L*} system through a more effective cage of TSC orbitals, further stabilized by the electron density switch from the new antibonding Ψ_{aa}^{TSC} orbital of {Cp′L_2L*} to the metal d_{yz} AO (Fig. 3F).

As discussed above, TSC is more effective in the case of L_2 = 'PP' than 'NN'. This is confirmed by comparing some complex formation reactions of the 16e two-legged piano stool Ru and Fe complexes. Although the selected types do not encompass all possible transformations, they highlight the importance of interligand interactions rather than separate ligand–metal interactions to the reactivity of the complexes. The donor ligands chosen vary in the nature of the respective donor orbital, from a simple lone-pair to π- and σ-bond orbitals.

3.3. The reactivity of the Cp′ML_2 complexes

3.3.1. Reaction with dinitrogen

First we focus on dinitrogen, which is quite a good donor [76,77]. $[RuCp(tmeda)]^+$ reacts indeed readily and quantitatively with gaseous N_2 at −90° to give $[RuCp(tmeda)(N_2)]^+$, although the complex is very weak. At ambient temperatures there is fast exchange between bound and free N_2. Furthermore, the geometry of the $[RuCp(tmeda)]^+$ moiety remains almost unchanged when N_2 is coordinated, i.e. there is no change from C_{2v} to C_s symmetry. If, in addition, Cp is replaced by Cp* the LUMO of $[Cp^*Ru(tmeda)]^+$ is raised and N_2 is not added any more [20]. The coordination of N_2 to $[CpRuPP]^+$, in contrast, is slightly favored through a notable participation of the lone pair of N_2 in the TSC interaction, especially for the bent configuration (forming high-lying Ψ_{aaa}^{TSC}, which interacts with d_{yz} as shown in Fig. 3F). According to the present DFT calculations, the end-on N_2 addition to $CpRu(PH_3)_2$ with liberation of 26.7 kcal mol^{-1} is energetically more favorable than that to $CpRu(NH_3)_2$ (20.0 kcal mol^{-1}). Experimentally it is found that N_2 is added even at room temperature giving $[CpRu(dippe)(N_2)]^+$. But this complex also is

labile and extremely air-sensitive in solution. Thus, N_2 is replaced by acetone to give [CpRu(Me_2CO)(dippe)][BPh_4] [78]. Apart from this, $[Cp^*Ru(dippe)(N_2)]^+$ is also known. On the other hand, TSC is weakened if in place of the 'PP' chelate ligand two separate phosphine ligands are present. In fact, there is only one pertinent complex known, viz $[Cp^*Ru(N_2)(PEt_3)_2][BPh_4]$, which is very labile and reacts even with trace amounts of dioxygen [24].

It is thus suggested that the reactivity differences between the 16e-complexes $[CpRuNN]^+$ and $[CpRuPP]^+$ are not solely due to different ground state structures. It can be shown by calculation that TSC between the orbitals of $\{CpL_n\}$ and N_2 is distinctly weaker in $[CpRuNN]^+$ than in $[CpRuPP]^+$. Changing the metal does, of course, not affect TSC in the {Cp′–LL–N_2} system. For the case of iron, due to the low-lying LUMO of $[CpFe(dippe)]^+$, complex formation with N_2 is favorable at room temperature giving the diamagnetic end-on dinitrogen complex $[CpFe(N_2)(dippe)]^+$. On the other hand, the higher LUMO in related $[Cp^*Fe(dippe)]^+$ is the reason for the unwillingness to uptake dinitrogen not even at a pressure of 5 atm [44]. Due to the absence of TSC stabilization in the nitrogen congeners, the complex of N_2 with $[Cp^*Fe(tmeda)]^+$ is unknown unless there is additional stabilization through strong σ-donors as in [Cp*Fe(tmeda)(Cl)] [79].

3.3.2. Reaction with other σ donors

With stronger σ-donors, the TSC in the {Cp′–LL–(lone pair of σ-donor)} system is much more pronounced giving rise to stable 18e counterparts. From DFT calculations, CO addition is stronger to $CpRu(PH_3)_2$ than to $CpRu(NH_3)_2$ (58.5 vs. 50.1 kcal mol^{-1}, which is more exothermic than the reaction with N_2 described above). It is found that $[RuCp(tmeda)]^+$ reacts readily with CO at low temperatures, even via a solid–gas reaction, to give $[RuCp(tmeda)(CO)]^+$ [20]. Similarly, CO and CN^tBu and other compounds are bound to $[CpRu(dippe)]^+$ or $[Cp^*Ru(dippe)]^+$ to give the corresponding adducts [78]. In general, the CpRu complexes are more reactive than the Cp*Ru relatives as has already been remarked along with the addition of dinitrogen. In the absence of kinetic data, it is often difficult to estimate relative reactivities of the unsaturated Ru complexes. In case of the iron complexes the situation is clearer since, owing to small singlet/triplet separations, ligand coordination is not seldom accompanied by spin interconversion [80]. In this event the change in spin state is a simple indicator of reactivity. The sensitivity of the singlet/triplet separation to even weak ligand effects allows hints to be obtained of interligand interactions.

18e-Complexes resulting from the association of the $[Cp^*Fe(dppe)]^+$ cation with acetone or triflate, viz $[Cp^*Fe(dppe)(OCMe_2)]^+$, and $[Cp^*Fe(dppe)(O-SO_2CF_3)]$, have been shown to exhibit paramagnetic behavior in the solid and solution states [22,43,81] Replacing the Cp* ligand by Cp raises the HOMO–LUMO gap and makes the low-spin state favorable. The complex $[CpFe(dppe)(OCMe_2)]^+$ is in all likelihood diamagnetic in solution [43], while, as said above, its Cp* analogue is paramagnetic. Similarly, the related complexes $[CpFe(dippe)(AN)]^+$ and $[Cp^*Fe(dippe)-(AN)]^+$ have been shown to be diamagnetic and paramagnetic, respectively [44]. However, this regularity is shaky, because of the energetic parity between the HOMO–LUMO gap and electron pairing. Both $[CpFe(dppe)(AN)]^+$ and $[Cp^*Fe(dppe)(AN)]^+$ are diamagnetic [44].

The shaky high-spin/low-spin balance was demonstrated by the $[Cp^*Fe(dppe)(H_2O)]^+$ complex, which is paramagnetic in THF solution but diamagnetic in the solid state, at least as the PF_6^- salt [43]. The optimized structures of the singlet and triplet states of $[CpFe(dpe)(H_2O)]^+$ ($dpe = H_2PCH_2CH_2PH_2$) [22] reveal differences in the conformation of the coordinated water ligand. In the high-spin case, the coordination of the oxygen atom is planar and the H_2O–Fe plane is perpendicular to the Cp ring, whereas in the low-spin case the oxygen of H_2O is sp^3-hybridized. The former conformation reflects the interaction between the p lone-pair of oxygen and the metal d_{xy} AO (Fig. 5A, see also Figure 4 in Ref. [22]). As a result of the filled–filled interaction the d_{xy} orbital is pushed up and forms a high-lying HOMO provoking the conversion into the high-spin state. If the HOMO–LUMO gap is large, the four-electron repulsion involved in the $\langle p|d_{xy}\rangle$ interaction is minimized by rotating the oxygen lone pair upon which the overlap is decreased. The oxygen pyramidalization also tends to minimize this overlap. For both $[CpFe(dpe)(H_2O)]^+$ and $[CpFe(dppe)(H_2O)]^+$ the singlet states are calculated to be the most stable [22].

3.3.3. Reactions with unsaturated compounds

The π orbital of unsaturated compounds such as alkenes and alkynes can act as a σ-donor. Thus, $[RuCp(tmeda)]^+$ readily coordinates, in solid–gas reactions at low temperatures, the gases $CH_2{=}CH_2$, $CHF{=}CH_2$, HC≡CH in the η^2-bonding mode [20]. Similary, $[CpRu(dippe)]^+$ and $[Cp^*Ru(dippe)]^+$ bind alkenes like C_2H_4 to give the corresponding adducts. While the parent complex is stable, the Cp* congener needs an ethylene atmosphere [78] in agreement with the aforementioned destabilizing influence of the Cp* ligand. Apart from thermally stable $[CpFe(P(OMe)_3)_2(MeO_2CC{\equiv}CCO_2Me)]PF_6$ [82] related iron half-sandwich complexes containing alkyne are little known. In all these complexes the π orbital of the unsaturated organic ligand is oriented orthogonal to the metal–Cp vector and is symmetrically bonded to the metal even in

the case of unsymmetric alkynes as in [CpFe(CO)-[P(OPh)$_3$](η^2-MeC≡CR)]SbF$_6$ [R = Me, Ph] [83]. This allows notable d→π* back donation to occur as can be inferred from the deformation of the C≡C–R angle. This effect is confirmed by DFT calculations on the acetylene addition to CpRu(PH$_3$)$_2$. The liberated energy of 29.9 kcal mol^{-1} is much higher than would be expected if acetylene were a σ donor only.

From a classical point of view, these complex formations could be taken to support the claim that Fe(II) and Ru(II) are borderline between hard and soft acids [84,85]. On the other hand, there are also notable cation-π interactions involving the hard alkali metal ions such as in metalated and non-metalated acetylenes [86], in [(allyl)$_2$Si(C$_5$H$_4$)$_2$Na] between the π-allyl system and the Cp–Na–Cp unit, or in the [Cp$_2$Na]–ethylene complex [87]. From the TSC point of view, both the π and π* orbitals can participate in the combined ligand TSC orbitals which form a cage around the metal center and thus contribute to the stability of the molecular construction (Fig. 7). Actually, the interactions between the TSC orbitals of {Cp′L$_2$} (Fig. 3) and the metal AO's are reinforced by the presence of another ligand in the new {Cp′L$_2$ (>C=C<)} system (Fig. 7), explainable in terms of the 'closed' character of the TSC orbitals' construction. In the present case, therefore, the hard/soft concept may be considered as merely reflecting the differences in the various TSC interactions.

The participation of both π and π* orbitals in the TSC activates the coordinated unsaturated molecule towards an attack by both nucleophiles and electrophiles [88]. Although the alkynes are usually rather unreactive towards nucleophiles in the free state, π-coordinated species are prone to form vinyl-metal derivates with the nucleophile in *trans* position. As another example, attack by hydride sources such as the borohydride ion on [CpFe(CO)$_2$(olefin)]$^+$ yields the alkyl compounds CpFe(CO)$_2$R. Activation of ethylene on coordination (as measured by the extent of the interaction between the hydride 1s orbital and the coordinated ethylene) is due to the fact that the ethylene π* orbital is considerably stabilized relative to the free state [89]. The

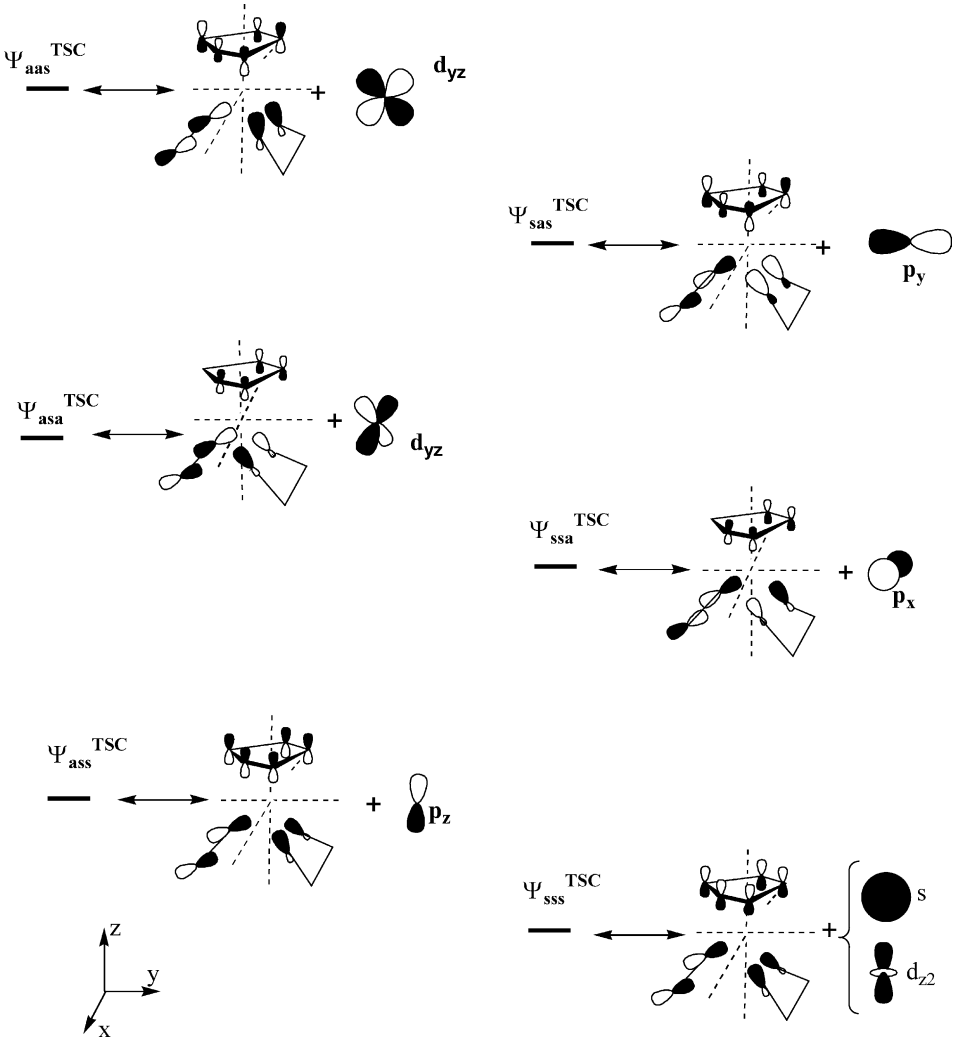

Fig. 7. Relevant TSC orbitals of the ligand system {Cp, L$_2$, C=C} and the metal AO's suitable for interaction in [CpM(L$_2$)(C=C)].

$[CpFeCO(L)(\eta^2\text{-alkyne})]BF_4$ [L = PPh_3, $P(OPh)_3$] complexes react with a wide variety of anionic nucleophiles to produce $CpFeCO(L)(\eta^1\text{-alkenyl})$ complexes [90] The reaction of $[CpFeCO(L)(\eta^2\text{-MeC}{\equiv}CMe)]BF_4$ [L = PPh_3, $P(OPh)_3$;] with nucleophilic reagents leads to a large variety of $CpFeCO(L)(\eta^1\text{-alkenyl})$ derivates. In all these cases the nucleophiles add *trans* [91]. Furthermore, terminal alkynes can be transformed into vinylidene complexes as in the reaction of $[RuCp(tmeda)]^+$ with HC≡CR (R = Bu^t, $SiMe_3$) [20]. The alkyne containing half-sandwich complexes $[CpFe(P(OMe)_3)_2(PhC{\equiv}CH)]PF_6$ or $[CpRu(PMe_3)_2(HC{\equiv}CH)]PF_6$ slowly transfom into the isomeric phenylvinylidene complexes [82].

3.3.4. Reaction with dihydrogen

The combination of the σ-accepting and π-donating properties of the $Cp'ML_2$ complexes under consideration creates the conditions for adding in the η^2 mode not only unsaturated compounds, but also the simple σ bond of dihydrogen. In other words, the replacement of the p-orbitals of the unsaturated molecule by the s orbitals of dihydrogen, does not change the general picture of the TSC orbitals in the $\{CpL_2H_2\}$ system depicted in Fig. 8. Therefore, the Cp complexes are again more reactive than the Cp* analogues. Whereas $[CpRu(tmeda)]^+$ reacts even in a solid–gas reaction readily with H_2 at low temperature to give $[RuCp(tmeda)(\eta^2\text{-}H_2)]^+$, which is thermally stable at temperatures about −70 °C [20], the more electron-rich $[Cp^*Ru(tmeda)]^+$ is unreactive under the same conditions [18,19]. This trend is also found in the chemistry of $[RuCp(PP)]^+$ and $[RuCp^*(PP)]^+$ [78,92–94].

The present DFT calculations show that the H_2 addition to $CpRu(PH_3)_2$ and $CpRu(NH_3)_2$ is exothermic by 21.9 and 12.7 kcal mol^{-1}, respectively. Thus the effect of L_2 is similar to that described above for the σ donor ligand addition. In the dihydrogen complexes, back donation via $d \rightarrow \sigma^*(H_2)$ electron transfer is strong and therefore the rotation of the $\eta^2\text{-}H_2$ ligand in $[Cp^*Ru(dppm)(H)_2]BF_4$ is hindered. In addition, the H–H distance of about 1.1 Å points to the presence of dihydrogen rather than dihydride [95]. The extent of back donation is increased through the participation of the $\sigma^*(H_2)$ orbital in the TSC orbitals of the $\{CpL_2H_2\}$ system (analogously to Ψ_{asa}^{TSC} and Ψ_{ssa}^{TSC} in Fig. 7). Lowering the $\sigma^*(H_2)$ orbital energy can ultimately complete the electron transfer to H_2 (oxidative addition) giving metal–hydride complexes such as $Cp'M(dip-(dippe)(H_2)$ (M = Ru or Fe). Similarly, conversion of $[Cp^*Ru(dppm)(\eta^2\text{-}H_2)]BF_4$ into the hydride complex

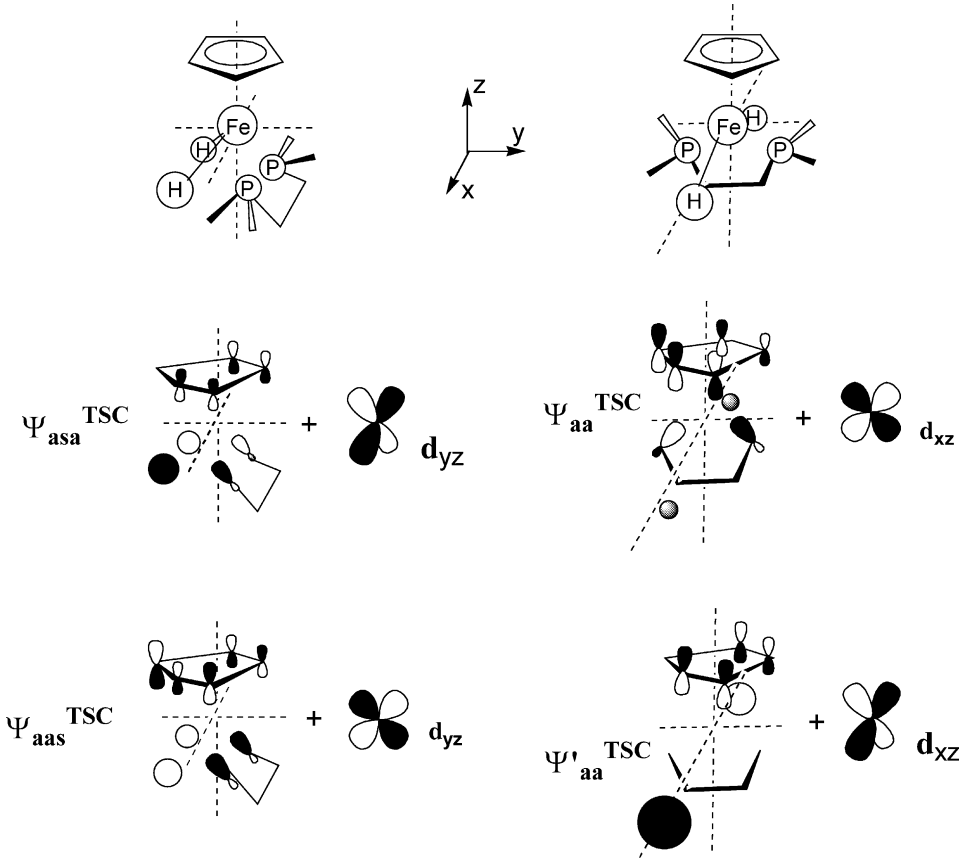

Fig. 8. Relevant TSC orbitals of the ligand system {Cp, L_2 H,H} and the metal AO's suitable for interaction in $CpM(H)_2(L_2)$ with *cis* (left side) and *trans* (right side) arrangement of the hydrids and L_2. Top: *cis*- and *trans* conformation of $CpFe(PP)(H)_2$.

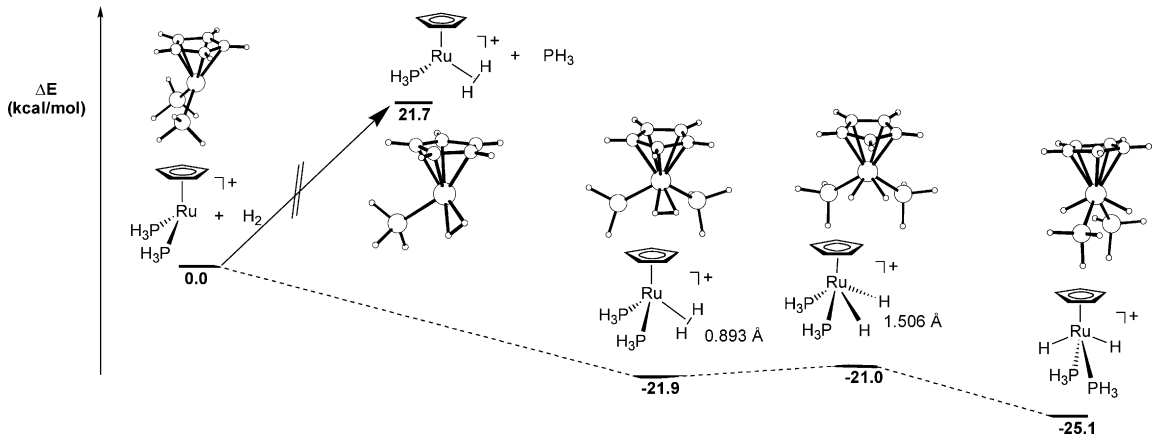

Fig. 9. Potential energy profiles of the addition of dihydrogen to $CpRu(PH_3)_2$.

$[Cp^*Ru(dppm)(H)_2]BF_4$ is fast at room temperature [95]. In all these cases, the hydride ligands adopt a transoid disposition [78,96]. In a 'PP' environment, both RuCp and RuCp* complexes react with H_2 to give the classical Ru(IV) dihydride complexes [78,92,93] as well as $[CpFe(H_2)(dippe)][BPh_4]$ and $[Cp^*Fe(dippe)(H_2)][BPh_4]$. These iron complexes may be regarded as organoiron(IV) species with a transoid arrangement of the hydride ligand, consistent with an Fe(IV) dihydride.

The DFT results for the model reaction $\{CpRu(PH_3)_2+H_2\}$ are depicted in Fig. 9. Accordingly, the formation of the dihydrogen complex is not preceded by the dissociation of a PH_3 ligand but instead occurs by an associative pathway. The initially formed dihydrogen complex converts slightly endothermically into the *cis*-dihydride complex, which then transforms into the *trans* isomer. This reaction pathway is confirmed experimentally in that several dihydrogen complexes of ruthenium $[Cp^*Ru(dppm)(H_2)]^+$, $[CpRu(dppe)(H_2)]^+$, $[CpRu(dmpe)(H_2)]^+$, $[Cp^*Ru(dppip)(H_2)]^+$, and $[Cp^*Ru(dmpm)(H_2)]^+$ are in equilibrium with the dihydride forms, which adopt a *transoid* capped four-legged piano stool structure [97].

The preference of the transoid disposition of the hydride ligands over cisoid is persuasive evidence of the TSC role played in the molecular geometry. In the case of *cis* arrangement of the 'PP' and hydride ligands, relevant for maximum interligand vdW attraction are the antibonding parts of the TSC interactions (Ψ_{asa}^{TSC} and Ψ_{aas}^{TSC} in Fig. 8, left). These orbitals are formed between each e1 (π_a of Cp) and the asymmetric or symmetric combination of the lone pairs of the P and H^- ligands and have C_1 symmetry, which allows coupling with the metal d_{yz} and d_{xz} AO's. Because of the energy difference between the lone pairs of P and H^-, the overlap population in the metal–ligand system is smaller than one with the *trans*-arrangement of 'PP' and hydride ligands. In the latter case the TSC interaction occurs between each e1 (π_a of Cp) and the asymmetric TSC orbital of the 'PP' or hydride ligands (Ψ_a^{TSC} or Ψ_a^{TSC} (H, H)), forming either the Ψ_{aa}^{TSC} orbital with 'PP' or Ψ'^{TSC}_{aa} with the hydrides (Fig. 8, right), with C_{2v} symmetry. Hence coupling with the metal d_{yz} and d_{xz} AO's is much stronger. With the nitrogen counterpart, DFT calculations show that the *cis* form of the $\{CpRu(NH_3)_2(H)_2\}$ hydride is not stable but back-transforms to the dihydrogen complex. This is a consequence of the absence of TSC (vide supra). Albeit the dihydrogen → hydride conversion is endothermic by 2.2 kcal mol^{-1}, the *trans* $\{CpRu(NH_3)_2(H)_2\}$ hydride is somewhat stabilized, as expected from the TSC concept.

It should be mentioned that the preference of the transoid disposition of the hydride ligands over cisoid critically depends on the TSC interactions involving the L_2 ligand. For example, in the DFT-optimized structure of the model system CpRu(amidinate) (amidinate = $(HN)_2CH^-$ anion) the N–C–N amidinate plane is not perpendicular to the Cp plane (cf Fig. 10, left structure), in line with the experimental Cp* relative [15]. The calculated inversion barrier of 3.1 kcal mol^{-1} is evidence in favor of appreciable TSC interactions between Cp and the π-allyl system of amidinate. If now H_2 is added, as outlined in Fig. 10, the *cis* dihydrid $[CpRu(amidinate)(H)_2]$ is 4.7 kcal mol^{-1} more stable than the *trans* isomer, due to TSC between π systems of Cp and π-allyl system of amidinate. But apart from this, in four-legged piano stool complexes, the chelate ligands are typically found in *trans* position owing to the TSC interactions between Cp and the chelate ligand such as in $Cp^*MoCl_2(dppe)$ [98] or due to TSC interactions between two chelate ligands, as was found in *trans*-$[Ru(dppe)_2(CO)(Cl)]$ [99]. In terms of the TSC concept such *trans* geometry is no longer unexpected.

3.3.5. Oxidative addition

The oxidative addition of H_2S or RSH to the ruthenium and iron complexes is a reaction borderline between the addition of σ donors and dihydrogen. The first step of reaction is simply the addition of the incoming ligand with formation of the 18e complexes

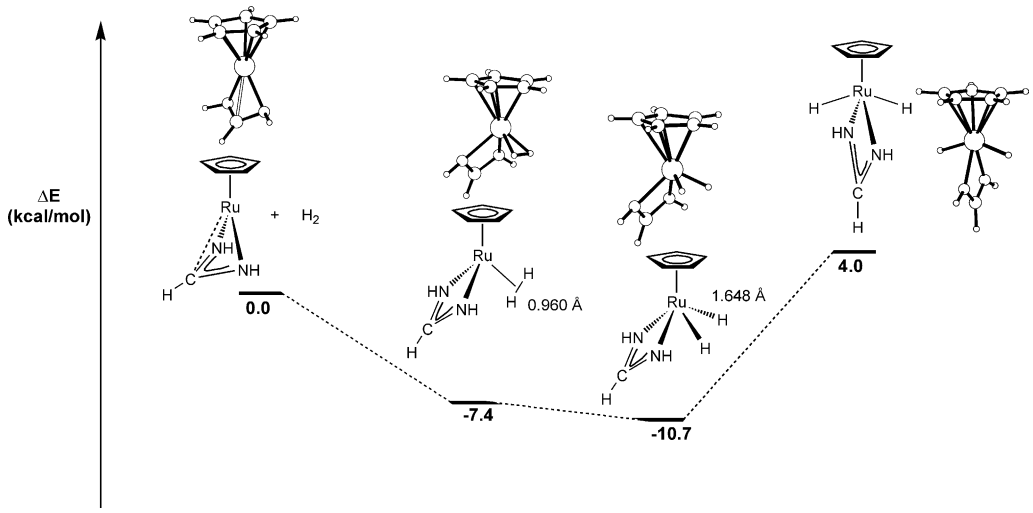

Fig. 10. Potential energy profiles of the addition of dihydrogen to CpRu(amidinate).

$CpML_2(HSR)$. A likely transition product is the extremely air-sensitive benzenethiol complex [CpRu(HSPh)(dippe)][BPh_4] [100]. Subsequent air oxidation affords the ruthenium(III) thiolate [CpRu(SPh)(dippe)][BPh_4]. In similar manner $[RuCp(dippe)]^+$ reacts with H_2S to give the binuclear disulfido derivate $[\{RuCp(dippe)\}_2(\mu\text{-}S_2)][BPh_4]_2$ [101]. Furthermore, $[CpFe(dppe)–SCH_2CH_2S–Fe(dppe)Cp](PF_6)_2$ results from reacting $[CpFe(dppe)]^+$ with $HS–CH_2CH_2–SH$ [102]. With biologically active RSH molecules (L-cysteine hydrochloride, dithiothereitol and 2-mercaptoethanol) the paramagnetic iron(III) thiolate complexes [CpFe(dppe)SR]PF_6 are afforded [103].

In comparing the differences in the Cp versus Cp* reactivity, it is worth noting that, while the complexes with Cp* are weaker acceptors as shown above, they are stronger donors favoring back-donation. For instance, the Cp* unit raises the filled metal AO's and thereby enhance the basicity of the metal in a series of complexes containing the Cp*Ru fragment by 5.5–9.0 kcal mol^{-1} over that of parent CpRu [104]. As a consequence, complete electron transfer M→ligand is reachable. Thus, $[Cp^*Ru(PEt_3)_2]$ undergoes oxidative addition of H_2S affording the Ru(IV) hydridothiol $[Cp^*RuH(SH)(PEt_3)_2]^+$ with *trans* orientation of the H and SH anions [100], similarly to the metal hydride complexes mentioned above. Likewise, [RuCp*(dippe)] (in situ) undergoes oxidative addition of H_2S affording the Ru(IV) hydridothiole $[RuCp^*H(SH)(dippe)]^+$ [101]. It is typically impossible to isolate intermediate products in the oxidative additions of Cp* complexes.

Clearly, the filling of the acceptor orbital in the d^6 complexes going to d^8 changes the acceptor property of 16 e complexes due to the replacement of symmetry and the LUMO energy level. The singlet–triplet crossing keep the symmetry of acceptor orbitals like in the unsaturated d^6 complexes. Therefore, for example, the weak vdW adduct of triplet $[Cp^*Ir(PR_3)]$ and ethylene probably is the key intermediate in the formation of the vinyl hydride $[Cp^*Ir(PMe_3)(CH{:}CH_2)H]$ [105].

3.3.6. Reaction with dioxygen

A particularly intriguing reaction is the oxidative addition of dioxygen because this is a spin forbidden process since Ru(II) has a singlet ground state. Notwithstanding this, $[RuCp(tmeda)]^+$ reacts readily with O_2 at temperatures below −30 °C giving $RuCp(tmeda)(O_2)]^+$ in essentially quantitative yield [20]. Unlike the reaction with N_2, in the present case the π-donor property of the starting complex is more important than its σ acceptor property. Therefore, dioxygen coordinates more strongly to complexes containing the ligands Cp* and 'PP' than Cp and 'NN'. In the complexes $Cp^*Ru(O_2)(dippe)^+$ and $Cp^*Ru(O_2)(PEt_3)_2$ BPh_4 [95] the dioxygen ligand is bound so tightly that it cannot be displaced by N_2 nor H_2 [106]. In view of the disposition of the active TSC orbitals, the structure of $[Cp^*Ru(O_2)(dppm)]BPh_4$ may be described as a three-legged piano stool with the O_2 and the two PPh_2 groups forming the legs [106], comparable with the dihydrogen counterpart $[Cp^*Ru(H_2)(dppm)]BF_4$ [107]. The dioxygen is symmetrically bonded to ruthenium with an O–O distance of 1.37 Å which is in between that of the superoxide anion in K_2O (1.28 Å) and H_2O_2 (1.46 Å). It is not clear at present whether these diamagnetic complexes should be described as d^5 Ru(III) superoxo or d^4 Ru(IV) peroxo [20], or better as a complex with singlet dioxygen. Note that the diamagnetic behavior is consistent with all three descriptions. The O_2 ligand is oriented in a fashion so as to maximize the d(Ru)–$\pi^*(O_2)$ bonding [108].

While the corresponding dioxygen complexes with iron are unstable, theoretical calculations favor an end-on binding of dioxygen [109] with only a one-electron

transfer. π-Back-bonding from Fe(III) into the O–O σ* orbital is unfavorable energetically [110]. Therefore, dioxygen complexes are typically binuclear: the reaction between $[Fe_2^{II}(-OH)_2(6\text{-}Me_3\text{–}TPA)_2]^{2+}$ (6-Me_3–TPA = tris(6-methyl-2-pyridylmethyl)amine) and O_2 to form $[Fe_2^{III}(-O)(-O_2)(6\text{-}Me_3\text{–}TPA)_2]^{2+}$ is accompanied by coordination of dioxygen (involving the formation of two Fe–O_{peroxo} bonds in possibly a 1,2 mode) with transfer of two electrons. A large negative activation entropy of -175 ± 20 J mol^{-1} K^{-1} is typical of an associative rate-limiting step [111].

In this connection some comments on the nature of dioxygen binding to Fe(III) are at place here, based on the few mononuclear η^2-peroxide–ferric complexes reported [112] Strong experimental and theoretical evidence support a side-on structure in the Fe(III)–EDTA–peroxide complex, which has the dioxygen ligand in *trans* position to the N ligands, signaling strong TSC between O_2 and the 'NN' fragment. This configuration is favored over a square pyramidal geometry with O_2 ligand in the apex, since in the latter case the O_2 ligand cannot participate in TSC. It may be noted that strong TSC supports the formation of strong, covalent bonds involving the Fe-d_{xy} and peroxide-π* orbitals, in line with spectroscopic evidence. According to DFT calculations, there is little contribution from π-symmetry iron–peroxide interactions. Such a side-on η^2 FeO_2 arrangement in terms of TSC should be taken in consideration also in the treatment of related heme and non-heme peroxo–iron complexes [113,114]. As claimed by Valentine and coworkers, the peroxo ligand in these complexes displays nucleophilic rather than electrophilic character, with nucleophilicity being modulated by the axial ligand. This idea is strongly supported by the present TSC scheme, since just the axial ligand is capable of creating TSC interactions.

4. Summary

Intracomplex attractive and repulsive forces between valence-saturated non-bonded atoms or atomic groups, modified by metal–ligand interaction, are a determinant of the geometry and properties of the two-legged piano stool complexes Cp′ML_2. The TSC concept offers a criterion with which to decide whether the complex has a planar or pyramidal structure, and whether it is diamagnetic or paramagnetic. The important parameter determining the spin state is the ratio of the electron pairing energy to the HOMO–LUMO gap.

The driving force for planar/pyramidal inversion involves strengthening of the interaction between the metal AO's and the TSC ligand orbitals via Ψ_{as}^{TSC} and Ψ_{aa}^{TSC} (Figs. 2 and 3), depending on the nature of L_2. Since the 'PP' ligands have more efficient TSC with Cp′ than 'NN', the increase in ΔE^{TSC} upon bending is more pronounced for the Cp–'PP' system. The enhanced mixing of the TSC orbitals contributes to the stabilization of the complex, and hence the Cp′–'PP' complexes are pyramidal in the ground state. On the other hand, the very weak TSC interactions in the amine complexes render the potential energy surface for the inversion very flat, and this favors the planar construction.

Changing the metal has, of course, little effect on TSC in the {Cp′–L_2–L*} system (where L* is the incoming ligand) and therefore the general picture of the interligand interactions is maintained. The spin state change often occurring with Fe(II) is the result of two effects: (i) it costs more energy to pair electrons in the smaller Fe 3d orbitals than in the more diffuse Ru 4d orbitals; and (ii) due to the lower electron affinity of Fe compared to Ru the interaction in the Fe–{Cp′–L_2–L*} system is weak resulting in a smaller HOMO–LUMO gap. In this respect, the diamagnetic and paramagnetic varieties reflect the intensity of the ligand–metal interaction rather than the complex geometry (planar or pyramidal).

For the chemical properties, the TSC interligand interaction affects the donor/acceptor behavior towards an incoming ligand. The relative contributions of both depend on the level and spatial orientation of the vacant orbitals LUMO (Fig. 6) and the set of filled HOMO, HOMO+1 and HOMO+2 (Fig. 5). The activity of these orbitals is guided by the new TSC ligand orbitals formed including both the donor and acceptor orbitals of the incoming ligand (Fig. 7). Of course, the 16e $[Cp'ML_2]^+$ complexes are better classified as acceptors than donors.

For the Cp versus Cp* reactivity difference, the energies of both the LUMO (which is mainly determined by the e1 orbital of Cp′ with minor contribution of L_2) and the set of HOMOs are raised in going from $CpML_2$ to Cp^*ML_2. This means that the former complexes are stronger acceptors but weaker donors than the Cp^*ML_2 counterparts. Therefore, the $CpML_2$ complexes have higher affinity for adding a σ ligand. The role of the co-ligands L_2 in this process is providing TSC orbitals that can strongly interact with suitable metal d AO's (Fig. 3F). Since the Cp′–'PP' TSC interaction is more effective than that in Cp′–'NN', the 'PP' complexes are more stable. The interactions between the TSC orbitals of {Cp′L_2} (Fig. 3) are reinforced by the presence of the added ligand in the new {Cp′L_2L*} system through a 'closed' TSC orbitals' construction (Fig. 7). This construction is destabilized, however, by the high-lying occupied antibonding TSC orbitals, but can be stabilized by shifting electron density to the metal. In this way vdW repulsion partly switches over into vdW attraction, minimizing electron–electron repulsion. It is this feature that ultimately provides the driving force of attack and the stability of the 18e-complex.

Finally, concerning the back donation behavior, Cp* favors the subsequent transformation of the added ligand towards an oxidative addition product. This is due to the participation of the π* orbitals of Cp′ in the combined ligand TSC orbitals and occurs with unsaturated compounds, dihydrogen, thiols and dioxygen. The effect of the TSC orbital involving the σ* or π* orbitals of the added ligand is typically mistaken for d → π* back donation.

5. Computational details

All calculations were performed using the GAUSSIAN-98 software package [115] on the Silicon Graphics Power Challenge of the Vienna University of Technology. The geometry and energy of all model complexes were optimized at the B3LYP level [116] with the Stuttgart/Dresden ECP (SDD) basis set [117] to describe the electrons of the ruthenium atom. For C and H the Dunnning–Huzinaga valence double-ξ basis set (D95v) was used [118], while for N and P a full double-ξ basis set with a polarization function (D95*) was employed. A vibrational analysis was performed to confirm that the compounds have no imaginary frequency. The geometries were optimized without constraints (C_1 symmetry). The extended Hückel calculations [119] were carried out with the CACAO program systems [120].

Acknowledgements

Financial support by the 'Fonds zur Förderung der wissenschaftlichen Forschung' (Project No. P14681-CHE) is gratefully acknowledged.

References

[1] I. Omae, Applications of Organometallic Compounds, Wiley-VCH, Chichester, 1998, p. 1ff.
[2] A.J. Pearson, Acc. Chem. Res. 3 (1980) 463.
[3] R. Poli, Chem. Rev. 96 (1996) 2135.
[4] H. Sitzmann, Coord. Chem. Rev. 214 (2001) 287.
[5] M. Laing, J. Chemical Education 78 (2001) 1400.
[6] C. Elschenbroich, R. Moeckel, A. Vasil'kov, B. Metz, K. Harms, Eur. J. Inorg. Chem. 10 (1998) 1391.
[7] Do Thic Ngoc Phan, S. Spichiger, P. Paglia, G. Bernardinelli, E.P. Kundig, P.L. Timms, Helv. Chim. Acta 75 (1992) 2593.
[8] J.A. Mata, E. Peris, J. Chem. Soc. Dalton Trans. (2001) 3634.
[9] T.R. Ward, O. Schafer, C. Daul, P. Hofmann, Organometallics 16 (1997) 3207.
[10] T.J. Johnson, K. Folting, W.E. Streib, J.D. Martin, J.C. Huffman, S.A. Jackson, O. Eisenstein, K.G. Caulton, Inorg. Chem. 34 (1995) 488.
[11] P.J. Fagan, W.S. Mahoney, J.C. Calabrese, I.D. Williams, Organometallics 9 (1990) 1843.
[12] U. Kölle, J. Kossakowski, N. Klaff, L. Wesemann, U. Englert, G. Herberich, Angew. Chem. Int. Ed. Engl. 30 (1991) 980.
[13] J. McGrady, Angew. Chem. Int. Ed. Engl. 39 (2000) 3077.
[14] K.-J. Haack, S. Hashiguchi, A. Fujii, T. Ikariya, R. Noyori, Angew. Chem. Int. Ed. Engl. 36 (1997) 285.
[15] Y. Yamaguchi, H. Nagashima, Organometallics 19 (2000) 725.
[16] P.J. Bailey, K.J. Grant, S. Parso, Organometallics 17 (1998) 551.
[17] K. Mashima, H. Kaneyoshi, S. Kaneko, A. Mikami, K. Tani, A. Nakamura, Organometallics 16 (1997) 1016.
[18] C. Gemel, K. Mereiter, R. Schmid, K. Kirchner, Organometallics 16 (1997) 5601.
[19] C. Gemel, V.N. Sapunov, K. Mereiter, M Ferencic, R. Schmid, K. Kirchner, Inorg. Chim. Acta 286 (1999) 114.
[20] C. Gemel, J.C. Huffman, K.G. Caulton, K. Mauthner, K. Kirchner, J. Organomet. Chem. 593–594 (2000) 342.
[21] K.G. Caulton, New. J. Chem. 18 (1994) 25.
[22] K. Costuas, J.Y. Saillard, Organometallics 18 (1999) 2505.
[23] S.E. Garner, A.G. Orpen, J. Chem. Soc. Dalton Trans. (1993) 533.
[24] M.J. Tenorio, M.C. Puerta, P.J. Valerga, J. Organomet. Chem. 609 (2000) 161.
[25] T.M. Jimenez, K. Mereiter, M.C. Puerta, P. Valerga, J. Am. Chem. Soc. 122 (2000) 11230.
[26] K.M. Smith, R. Poli, P. Legzdins, Chem. Eur. J. 5 (1999) 1598.
[27] K.M. Smith, R. Poli, P. Legzdins, Chem. Commun. (Cambridge) 17 (1998) 1903.
[28] C.C. Bickford, T.J. Johnson, E.R. Davidson, K.G. Caulton, Inorg. Chem. 33 (1994) 1080.
[29] B.K. Campion, R.H. Heyn, D.D. Tilley, J. Chem. Soc. Chem. Commun. (1988) 278.
[30] U. Kölle, J. Kossakowski, G. Raabe, Angew. Chem. Int. Ed. Engl. 29 (1990) 773.
[31] U. Kölle, C. Rietmann, G. Raabe, Organometallics 16 (1997) 3273.
[32] T. Arliguie, C. Border, B. Chaudret, J. Devillers, R. Poilblanc, Organometallics 8 (1989) 1308.
[33] E. Lindner, M. Haustein, H.A. Mayer, K. Gierling, R. Fawzi, M. Steinmann, Organometallics 14 (1995) 2246.
[34] T.J. Johnson, J.C. Huffman, K.G. Caulton, J. Am. Chem. Soc. 114 (1992) 2725.
[35] T. Braun, M. Laubender, O. Gevert, H. Werner, Chem. Ber. Recueil 130 (1997) 559.
[36] J. Huang, H.-J. Schanz, E.D. Stevens, S.P. Nolan, Organometallics 18 (1999) 2370.
[37] J. Huang, E.D. Stevens, S.P. Nolan, J.L. Petersen, J. Am. Chem. Soc. 121 (1999) 2674.
[38] J. Huang, L. Jafarpour, A.C. Hillier, E.D. Stevens, S.P. Nolan, Organometallics 200 (2001) 2878.
[39] M. Cao, L.V. Do, N.W. Hoffman, M.-L. Kwan, J.K. Little, J.M. McGilvray, C.B. Morris, B.C. Söderberg, A. Wierzbicki, T.R. Cundari, C.H. Lake, E. Valente, J. Organomet. 20 (2001) 2270.
[40] D.L. Davies, J. Fawcett, S.A. Garratt, D.R. Russell, Organometallics 20 (2001) 3029.
[41] H. Sitzmann, T. Dezember, W. Kaim, F. Baumann, D. Stalke, J. Kärcher, E. Dormann, H. Winter, C. Wachter, M. Kelemen, Angew. Chem. Int. Ed. Engl. 35 (1996) 2872.
[42] U. Siemeling, U. Vorfeld, B. Neumann, H.-G. Stammler, Organometallics 17 (1998) 483.
[43] P. Hamon, L. Toupet, J.-R. Hamon, C. Lapinte, Organometallics 15 (1996) 10.
[44] A. de la Jara Leal, M.J. Tenorio, M.C. Puerta, P. Valerga, Organometallics 14 (1995) 3839.
[45] J.R. Bleeke, R.J. Wittenbrink, T.W. Clayton, Jr., M.Y. Chiang, J. Am. Chem. Soc. 112 (1990) 6539.
[46] R.J. Lavallee, C. Kutal, J. Organomet. Chem. 562 (1998) 97.
[47] H. Takahashi, T. Ando, M. Kamigaito, M. Sawamoto, Macromolecules 32 (1999) 3820.
[48] V.N. Sapunov, K. Kirchner, R. Schmid, Coord. Chem. Rev. 214 (2001) 143.

[49] J. Eloranta, V.A. Apkarian, J. Chem. Phys. 115 (2001) 752.
[50] S.M. Cybulski, R.R. Toczyowski, J. Chem. Phys. 111 (1999) 10520.
[51] M.R. Flannery, K.J. McCann, N.W. Winter, J. Chem. Phys. Sect. B 14 (1981) 3789.
[52] S. Okajima, P.C. Subudhi, E.C. Lim, J. Chem. Phys. 65 (1977) 4611.
[53] (a) N.E. Blank, M.W. Haenel, Chem. Ber. 114 (1981) 1520;
(b) N.-E. Blank, M.W. Haenel, Chem. Ber. 114 (1981) 1531.
[54] M.W. Haenel, D. Schweitzer, Adv. Chem. Ser. 217 (1988) 333.
[55] M. Munakata, J.C. Zhong, T Kuroda-Sowa, M. Maekawa, Y. Suenaga, M. Kasahara, H. Konaka, Inorg. Chem. 40 (2001) 7087.
[56] M. Masahiko, H. Naoki, K.-S. Takayoshi, S.Y.M. Megumu, Inorg. Chim. Acta 328 (2002) 254.
[57] P. Jutzi, Chem. Rev. 99 (1999) 969.
[58] S.C. Sockwell, T.P. Hanusa, Inorg. Chem. 29 (1990) 76.
[59] P. Comba, T. Gyr, Eur. J. Inorg. Chem. (1999) 1787.
[60] D.J. Burkey, T.P. Hanusa, J. Organometal. Chem. 512 (1996) 165.
[61] R.G. Pearson, Inorg. Chem. 27 (1988) 734.
[62] C. Dohmeier, H. Schnöckel, C. Robl, U. Schneider, R. Ahriches, Angew. Chem. Int. Ed. Engl. 32 (1993) 1665.
[63] M. Ito, M. Hirakawa, K. Murata, T. Ikariya, Organometallics 20 (2001) 379.
[64] H. Felkin, P.J. Knowles, B. Meunier, A. Mitschler, L. Ricard, R. Weiss, J. Chem. Soc. Chem. Commun. (1974) 44.
[65] J.M. Burlitch, S.E. Hayes, G.E. Whitwell, Organometallics 1 (1982) 1074.
[66] R.B. Petersen, J.M. Ragosta, G.E. Whitwell, J.M. Burlitch, Inorg. Chem. 22 (1983) 3407.
[67] E. Hey-Hawkins, H.-G. von Schnering, Z. Naturforsch. Teil. B 46 (1990) 621.
[68] (a) K. Jonas, L. Schiferstein, Angew. Chem. Int. Ed. Engl. 18 (1979) 549;
(b) K. Jonas, L. Schiferstein, Angew. Chem. Int. Ed. Engl. 18 (1979) 550;
(c) J. Jonas, Adv. Organomet. Chem. 19 (1981) 97;
(d) K. Jonas, Angew. Chem. Int. Ed. Engl. 24 (1985) 295.
[69] P. Rosa, L. Ricard, F. Mathey, P. Le Floch, Organometallics 19 (2000) 5247.
[70] F.R. Lemke, K.J. Galat, W.J. Youngs, Organometallics 18 (1999) 1419.
[71] F.P. Arnold, Jr., Organometallics 18 (1999) 4800.
[72] R. Denis, L. Toupet, F. Paul, C. Lapinte, Organometallics 19 (2000) 4240.
[73] W.A. Schenk, U. Karl, M.R. Horn, S. Muessig, Chem. Sci. 45 (1990) 239.
[74] L. Cavallo, T.K. Woo, T. Ziegler, Can. J. Chem. 76 (1998) 1457.
[75] J.D. Atwood, T.L. Brown, J. Am. Chem. Soc. 98 (1974) 3160.
[76] G. Trimmel, C. Slugovc, P. Wiede, K. Mereiter, V.N. Sapunov, R. Schmid, K. Kirchner, Inorg. Chem. 36 (1997) 1076.
[77] R.J. Deeth, S.A. Langford, J. Chem. Soc. Dalton Trans (1995) 1.
[78] I. de los Rios, M.J. Tenorio, J. Padilla, P.M. Carmen, P. Valerga, Organometallics 15 (1996) 4565.
[79] K. Jonas, P. Klusmann, R. Goddard, Z. Naturforsch. Teil. B: Chem. Sci. 50 (1995) 394.
[80] J.L. Detrich, O.M. Reinaud, L.R. Rheingold, K.H. Theopold, J. Am. Chem. Soc. 117 (1995) 11745.
[81] P. Hamon, L. Toupet, J.-R. Hamon, C. Lapinte, J. Chem. Soc. Chem. Commun. (1994) 931.
[82] H. Schumann, G. Admiraal, P.T. Beurskens, Z. Naturforsch. Teil. B: Chem. Sci. 47 (1992) 1125.
[83] D.L. Reger, S.A. Klaeren, L. Lebioda, Organometallics 7 (1988) 189.
[84] F. Basolo, R.G. Pearson, Mechanism of Inorganic reactions, A Study of Metal Complexes in Solution, John Wiley & Sons, Inc, New York, London, Sydney, 1967, p. 25.
[85] P.E. Hoggard, G.B. Porter, J. Inorg. Nucl. Chem. 43 (1981) 185.
[86] B. Goldfuss, P. Schleyer, P. von Rague, F. Hampel, J. Am. Chem. Soc. 119 (1997) 1072.
[87] S. Harder, M. Lutz, S.J. Obert, Organometallics 18 (1999) 1808.
[88] P.J. Stang, F. Diederich, Modern Acetylene Chemistry, VCH, Weinheim, 1995, p. 107–108.
[89] A.D. Cameron, V.H. Smith, Jr., M.C. Baird, Int. J. Quantum Chem. Quantum Chem. Symp. 20 (1986) 657.
[90] D.L. Reger, Acc. Chem. Res. 21 (1988) 229.
[91] D.L. Reger, K.A. Belmore, E. Mintz, P. McElligott, J. Organomet. 3 (1984) 134.
[92] G. Jia, C.P. Lau, J. Organomet. Chem. 565 (1998) 37.
[93] G. Jia, R.H. Morris, J. Am. Chem. Soc. 113 (1991) 875.
[94] F.M. Conroy-Lewis, S.J. Simpson, J. Organomet. Chem. 322 (1987) 221.
[95] G. Jia, A.J. Lough, R.H. Morris, Organometallics 11 (1992) 161.
[96] T.M. Jimenez, M.C. Puerta, P. Valerga, Organometallics 13 (1994) 3330.
[97] J.K. Law, H. Mellows, D.M. Heinekey, J. Am. Chem. Soc. 124 (2002) 1024.
[98] J.C. Fettinger, D.W. Keogh, B. Pleune, R. Poli, Inorg. Chim. Acta 261 (1997) 1.
[99] L.F. Szczepura, J. Giambra, R.F. See, H. Lawson, T.S. Janik, A.J. Jircitano, M.R. Churchill, K.J. Takeuchi, Inorg. Chim. Acta 239 (1995) 77.
[100] A. Coto, M.J. Tenorio, M.C. Puerta, P. Valerga, Organometallics 17 (1998) 4392.
[101] A. Coto, I. de los Rios, M.J. Tenorio, M.C. Puerta, P. Valerga, J. Chem. Soc. Dalton Trans. 24 (1999) 4309.
[102] C. Diaz, Bol. Soc. Chil. Quim. 43 (1998) 477.
[103] C. Diaz, A. Pesce, Appl. Organomet. Chem. 14 (2000) 557.
[104] M.K. Rottink, R.J. Angelici, J. Am. Chem. Soc. 115 (1993) 7267.
[105] K.M. Smith, R. Poli, J.N. Harvey, Chem. Eur. J. 7 (2001) 1679.
[106] G. Jia, W.S. Ng, H.S. Chu, W. Wing-Tak, Yu Nai-Teng, I.D. Williams, Organometallics 18 (1999) 3597.
[107] W.T. Klooster, T.F. Koetzle, G. Jia, T.P. Fong, R.H. Morris, A. Albinati, J. Am. Chem. Soc. 116 (1994) 7677.
[108] B.E.R. Schilling, R. Hoffmann, D.L. Lichtenberger, J. Am. Chem. Soc. 101 (1979) 585.
[109] A.L. Feig, S.J. Lippard, Chem. Rev. 94 (1994) 759.
[110] J. Du Bois, T.J. Mizoguchi, S.J. Lippard, Coord. Chem. Rev. 200–202 (2000) 443.
[111] S.V. Kryatov, E.V. Rybak-Akimova, V.L.L. MacMurdo Que, Jr., Inorg. Chem. 40 (2001) 2220.
[112] F. Neese, E.I. Solomon, J. Am. Chem. Soc. 120 (1998) 12829.
[113] (a) M.F. Sisemore, J.N. Burstyn, J.S. Valentine, Angew. Chem. Engl. Ed. 35 (1996) 206;
(b) M. Selke, M.F. Sisemore, J.S. Valentine, J. Am. Chem. Soc. 118 (1996) 2008;
(c) M.F. Sisemore, M. Selke, J.N. Burstyn, J.S. Valentine, Inorg. Chem. 36 (1997) 979;
(d) M. Selke, J.S. Valentine, J. Am. Chem. Soc. 120 (1998) 2652.
[114] (a) E. McCandlish, A.R. Miksztal, M. Nappa, A.Q. Sprenger, J.S. Valentine, J.D. Stong, T.G.J. Spiro, Am. Chem. Soc. 102 (1980) 4268;
(b) A.R. Miksztal, J.S. Valentine, Inorg. Chem. 23 (1984) 3548;
(c) J.N. Burstyn, J.A. Roe, A.R. Miksztal, B.A. Shaevitz, G. Lang, J.S. Valentine, J. Am. Chem. Soc. 110 (1988) 1382;
(d) S. Ozawa, Y. Watanabe, I. Morishima, Inorg. Chem. 33 (1994) 306;
(e) M.H. Dickman, M.T. Pope, Chem. Rev. 94 (1994) 569;
(f) P. Friant, J. Goulden, J. Fischer, L. Ricard, M. Schappacher, R. Weiss, M. Momentou, Nouv. J. Chim. 9 (1985) 33.

[115] M.J. Frisch, G.W. Trucks, H.B. Schlegel, G.E. Scuseria, M.A. Robb, J.R. Cheeseman, V.G. Zakrzewski, J.A. Montgomery, Jr., R.E. Stratmann, J.C. Burant, S. Dapprich, J.M. Millam, A.D. Daniels, K.N. Kudin, M.C. Strain, O. Farkas, J. Tomasi, V. Barone, M. Cossi, R. Cammi, B. Mennucci, C, Pomelli, C. Adamo, S. Clifford, J. Ochterski, G.A. Petersson, P.Y. Ayala, Q. Cui, K. Morokuma, D.K. Malick, A.D. Rabuck, K. Raghavachari, J.B. Foresman, J. Cioslowski, J.V. Ortiz, B.B. Stefanov, G. Liu, A. Liashenko, P. Piskorz, I. Komaromi, R. Gomperts, R.L. Martin, D.J. Fox, T. Keith, M.A. Al-Laham, C.Y. Peng, A. Nanayakkara, C. Gonzalez, M. Challacombe, P.M.W. Gill, B.G. Johnson, W. Chen, M.W. Wong, J.L. Andres, M. Head-Gordon, E.S. Replogle, J.A. Pople, GAUSSIAN-98, revision A.5; Gaussian, Inc., Pittsburgh, PA, 1998.

[116] (a) A.D. Becke, J. Chem. Phys. 98 (1993) 5648; B. Miehlich, A. Savin, H. Stoll, H. Preuss, Chem. Phys. Lett 157 (1989) 200.;
(b) C. Lee, W. Yang, G. Parr, Phys. Rev. Sect. B 37 (1988) 785.

[117] (a) U. Haeusermann, M. Dolg, H. Stoll, H. Preuss, Mol. Phys. 78 (1993) 1211;
(b) W. Kuechle, M. Dolg, H. Stoll, H. Preuss, J. Chem. Phys. 100 (1994) 7535;
(c) T. Leininger, A. Nicklass, H. Stoll, M. Dolg, P. Schwerdtfeger, J. Chem. Phys. 105 (1996) 1052.

[118] T.H. Dunning, P.J. Hay, in: H.F. Schäfer, III (Ed.), Modern Theoretical Chemistry, Plenum Press, New York, 1976, pp. 1–28.

[119] (a) R. Hoffmann, W.N. Lipscomb, J. Chem. Phys. 36 (1962) 2179;
(b) R. Hoffmann, J. Chem Phys. 39 (1963) 1397;
(c) J.H. Ammeter, H.-B. Bürgi, J.C. Thibeault, R. Hoffmann, J. Am. Chem. Soc. 100 (1978) 3686.

[120] C. Mealli, D.M. Proserpio, J. Chem. Educ. 67 (1990) 399.